

---

---

U.S.D.A. FOREST SERVICE  
RESEARCH PAPER  
FPL 139  
JULY 1970

---

u.s. department of agriculture | forest service | forest products laboratory | madison, wisconsin

---

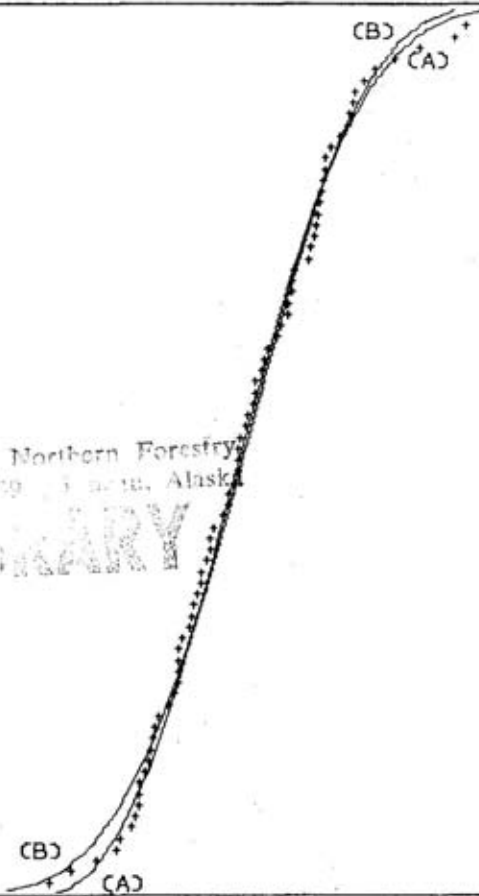
# STRENGTH OF MULTIPLE - MEMBER STRUCTURES

---

---

Institute of Northern Forestry  
P. O. Box 909 Fairbanks, Alaska

LIBRARY



---

## ***abstract***

---

The variability in strength characteristic of lumber gives rise to structures in which both strong and weak members act in parallel to support the load. However, it is the present practice to design these multiple-member wood structures as if they consisted entirely of replicates of the weakest member permitted in the grade. This results in a low efficiency of lumber utilization. Furthermore, the low probability of such a structure ever occurring suggests that the allowable design stress could safely be raised if we understood the effects of random selection of members from a variable population. A tentative ASTM standard, D 2018, was written as the basis for a load-sharing increase in allowable unit stresses but was ultimately allowed to expire for lack of research data to support it. Variability has made it difficult to produce conclusive experimental evidence for load-sharing, although evidence exists to suggest that it is a valid concept. Lumber grading agencies, standards agencies, and code officials have long been interested in the question.

The present research is of a theoretical nature and is limited by its simplifying assumptions. For example, the structure chosen for study has only a single deck element at midspan. However, the objective was merely to gain insight into the effects of joining beams with a load-distributing element. Attention was focused on effects associated with random selection of beams from a variable population. These are the effects which are most difficult to study experimentally.

Four sets of strength and stiffness data, obtained from grade surveys, were used as input information. In all four cases, a rigid deck element was found to raise the apparent strength by about 12 percent compared to that of structures with no deck to redistribute the load. The load-sharing effect is thus seen to be small in this type of structure, indicating that caution is required in the upward adjustment of allowable unit stresses.

The theory developed and presented here is of permanent value. It combines statistical and mechanical concepts and could be applied to other areas such as the effect of size upon strength and structural reliability analysis.

---

---

# **STRENGTH OF MULTIPLE – MEMBER STRUCTURES<sup>1</sup>**

---

*JOHN J. ZAHN, Engineer*

---

*Forest Products Laboratory <sup>2</sup>  
Forest Service  
U.S. Department of Agriculture*

---

---

## ***introduction***

---

Wood-frame structures are designed on the basis of allowable stresses which are set low enough that about 95 percent of the members found in a given lumber grade are able to carry the full design load safely. This is equivalent to assuming that the structure is of the weakest-link type, that is, one whose load capacity is governed by the strength of its weakest member. The extra strength of other members, which may be several times stronger than the weakest one owing to the variability of wood, is effectively wasted and treated as unavailable to the structure.

But is this extra strength in fact unavailable? Not if it is postulated that weaker members have enough deflection capacity to deflect out of the way while their stiffer and stronger neighbors assume a greater share of the load. It is a well known principle of structural analysis that stiffer members carry a greater share of the load in statically indeterminate structures. Since in wood floors and roofs stiffer members tend to be stronger as well, it is reasonable to assume that the stronger members carry more than an equal share of the load. This is the wood industry's concept of a "load sharing" system.

For the purposes of this study, load sharing shall be defined as the embodiment of the following effects: (1) reduction in effective variability due to grouping of individual members into structures (grouping); (2) increase in effective strength due to joining of members into an indeterminate structure (mutual constraints); and (3) increase in effective strength due to increase in effective homogeneity whenever zones with defects are locally reinforced by neighboring members

---

<sup>1</sup>This research was supported in part by the Western Wood Products Association. Portland, Oreg., whose cooperation is gratefully acknowledged.

<sup>2</sup>Maintained at Madison, Wis., in cooperation with the University of Wisconsin.

(local reinforcement of defects). Only the first two of these effects were treated in this study. Mechanical effects such as T-beam action are not considered here as part of load sharing,

Effect (1) occurs whether members are joined or not. It is a size effect, i.e., the more material a structure contains, the more likely it is to contain a representative sample of material. Hence large structures tend to be more alike in their behavior than individual members of those structures. Effect (2) is due to the fact that joining members alters the mode of failure. It is the effect of primary interest in this study. Effect (3) is a local effect and hence concerns within-member variability whereas (1) and (2) concern between-member variability. This makes it a difficult effect to model theoretically since the required input information is not available. Therefore effect (3) was not treated.

Load sharing is unquestionably a sound concept in certain applications, such as the nailed vertically laminated beam, in which the third effect is assuredly present (3, 4, 5).<sup>3</sup> But its application to beam and deck structures such as wood floors and roofs is currently under challenge. Neighboring beams are felt to be too far away to provide local reinforcement of defects and the effect of mutual constraints is distrusted because it is not well understood. Therefore this research was undertaken to clarify the effect of mutual constraints upon the load capacity of wood floors and roofs. For this reason the study was restricted to beam and deck structures under uniform load.

#### Literature Review

Most of the studies of load-sharing systems reported in the literature consider only stiffness and do not consider strength. An exception is the work of Bonnicksen (3,4,5) on vertically laminated nailed beams. He found the minimum strength of 100 Douglas-fir 2 by 6 triplets to be 3,136 p.s.i. (pounds per square inch), whereas the minimum strength of one hundred 2 by 6 singlets was only 1,280 p.s.i. He noted a slight reduction in mean strength and a sharp reduction in variability due to vertical laminating. In unpublished work at the Forest Products Laboratory, Wayne Lewis considered three experimental floors under dead load; one of them failed suddenly and completely through all joists at a load only 22 percent greater than its design load. The most complete strength study has been done at the Forest Research Laboratory of Oregon State University (1) and the final report is not yet published.

Stiffness characteristics have been studied by several people. Williston and Abner (14) provide some measures of change in performance as construction procedures are changed, i.e., the effect of cross bracing, headers, subfloor, etc. They report a 40 percent decrease in deflection for a particular well-fastened floor system when compared with plywood sheets lying unfastened over joists. Additional information on stiffness of floor systems can be found in work by Russell (11) and the National Association of Home Builders (10).

---

<sup>3</sup>Underlined numbers in parentheses refer to Literature Cited on page 30.

## Approach

This research study employed the following approach: Weakest-link systems and brittlest-link systems were analyzed statistically and their load capacities compared. The brittlest-link system is one in which all members are constrained to deflect alike and the brittlest (one with the least deflection capacity) fails first. This represents the ideal mutual constraint afforded by an infinitely rigid deck.

Finally, a check was made on the conjecture that weakest-link and brittlest-link structures represent lower and upper bounds on the load capacity obtainable with a flexible deck. Since this was too complicated to be analyzed in closed form, a computer simulation technique was employed and the conjecture was not denied. It is reasonable to assume that the increased load capacity of brittlest-link systems (ideal load-sharing systems) over weakest-link systems represents the maximum benefit attainable from this randomly produced effect. The benefit of such mechanical effects as T-beam action would exist in addition to this.

Mechanical effects were not treated here because they are much easier to understand and to analyze than the probabilistic effects considered, and because it was hoped that some load-sharing benefits could be justified without reference to the strength of the deck or the stiffness of its fasteners. It should be pointed out that experimental data (1) show load capacity increases over weakest-link theory beyond what can be accounted for mechanically.

---

## ***method of investigation***<sup>4</sup>

---

The prototype structure shown in figure 1 was used to represent the essential features of a beam and deck structure. It consists of  $N$  simply supported beams bridged at midspan by a single deck element which is uniformly loaded. For the weakest-link structure, the deck element was assumed to be perfectly flexible; that is, each beam would carry an equal share of the total load. For the brittlest-link structure the deck element was assumed to be infinitely rigid, that is, each beam had the same center deflection and the beam with the least deflection capacity would fail first. This prototype deliberately omits any material contribution of the deck to the overall structure, so that the analysis exhibits only stochastic effects; that is, effects associated with the random selection of beams from a population with given strength and deflection capacity distributions. Two effects embodied in the load-sharing concept were modeled in the chosen prototype:

- (1) grouping into groups of  $N$
- (2) joining through a mutual constraint

Figure 2 shows a block diagram of the solution method. The input population was lumber of a given size, grade, and species, for which a bivariate  $P - \delta$  distribution was obtained by destructive strength testing of a representative sample, where  $P$  = strength (load at failure) and  $\delta$  = deflection capacity (deflection at failure). Figure 3 shows a typical load-deflection curve obtained from a

---

<sup>4</sup>A summary of the notation used in this report is included as Appendix D.

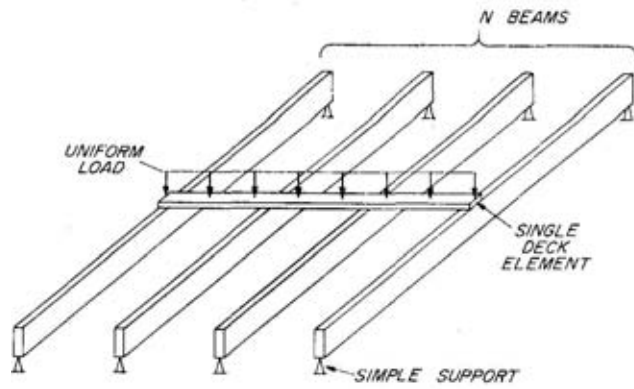


Figure 1.--Prototype structure.  
M 136 665

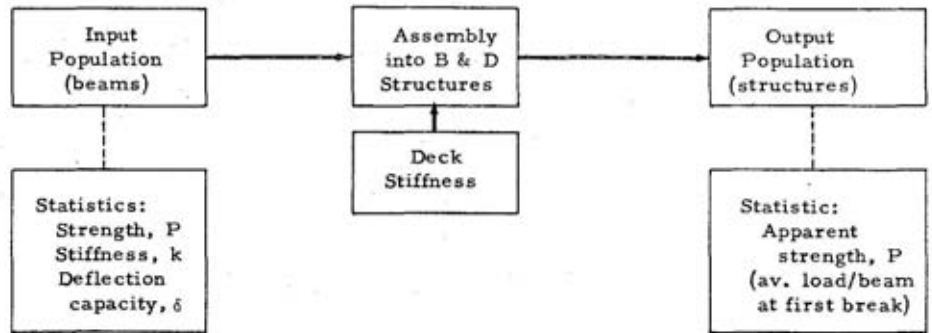


Figure 2.--Block diagram of solution method

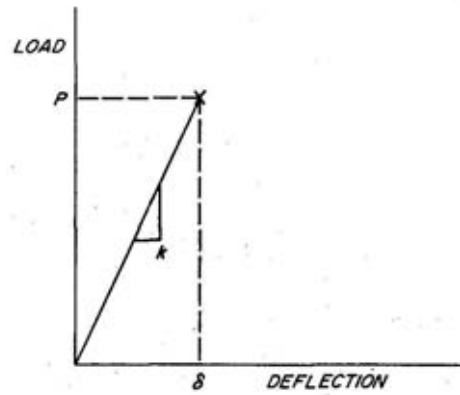


Figure 3.--Typical test of a low-grade beam.  
M 136 667

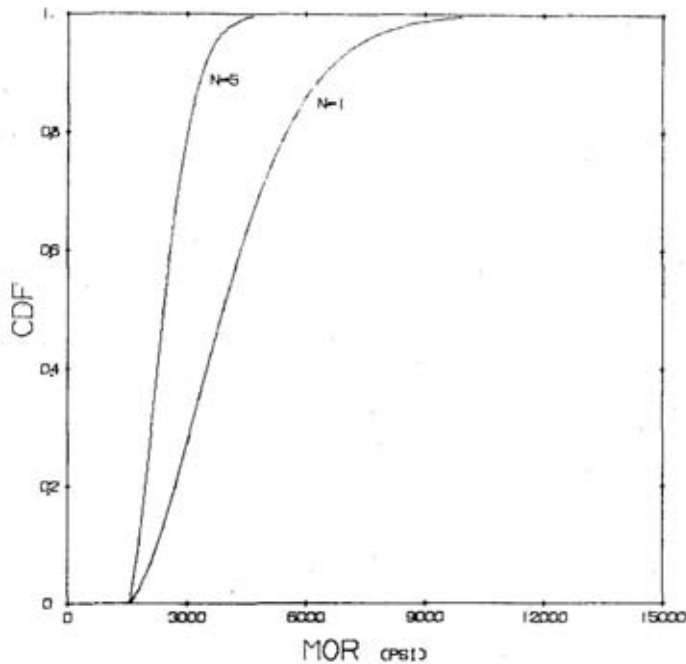


Figure 4.--Effect of grouping  
(size effect) in weakest-link  
structures of Grade 3 southern  
2 x 8's. M 136 646

bending strength test. It is assumed to be linear to failure. This is a reasonable assumption for relatively low-grade lumber since it fails at a local defect while still in the linear elastic range. Load sharing is of less interest when a high grade of lumber is used, because stiffness ordinarily governs the design of wood structures whenever higher strength material is employed. The slope of the curve,  $\underline{k}$ , is a measure of member stiffness. The three statistics  $\underline{P}$ ,  $\underline{k}$ , and  $\underline{\delta}$  are thus not independent but are related by the formula

$$P = k \delta \quad (1)$$

and only two of them need be recorded in a bending strength test. The numerical values actually reported by experimenters are the modulus of rupture (MOR) which is proportional to  $\underline{P}$  and the modulus of elasticity (MOE) which is proportional to  $\underline{k}$ . Hence, in the application of this analysis to populations of real beams, MOR was used as representative of  $\underline{P}$  and MOE as representative of  $\underline{k}$ . This scaling of the variables  $\underline{P}$  and  $\underline{k}$  has no effect on the comparisons of structures from the same input population.

The assembly of beams into structures may be thought of as an operator which transforms the input population of beams into an output population of structures. Associated with this is a mathematical operator, derived in the appendix, which transforms the input distributions into an output distribution. The output statistic of interest is the apparent strength,  $\underline{P}$ , defined as the total load at first break divided by  $\underline{N}$ , the number of beams. Thus, for weakest-link structures, the output  $\underline{P}$  is the strength of the weakest beam. For brittlest-link structures,  $\underline{P}$  is not necessarily the load on any particular beam but is rather the average of all the beam loads in the structure when the critical deflection of one of them has been reached. For this reason, it is called the "apparent" strength.

Failure of the structure was taken to be the load at which the first beam breaks, If the deck is sufficiently strong, this may not be the ultimate load capacity. Nevertheless, first break often is the ultimate, particularly under dead load, so for simplicity it is used as the criterion of failure,

In comparing the strength statistics of two populations, the entire cumulative distribution function (CDF) was employed rather than any single point value such as the mean or the mode or the 5 percent exclusion limit. The CDF of  $\underline{P}$  is by standard definition the fraction of the population whose strength is less than or equal to the argument,  $\underline{P}$ .

Table 1 shows a comparison of weakest-link and brittlest-link structures.

Table 1.--Comparison of structure types

Type of structure	Deck stiffness	All beams have same	Effects modeled
Weakest-link	Zero	Load	(1) grouping
Brittlest-link	Infinity	Midspan deflection	(1) grouping (2) common-deflection constraint

Note that both types include the effect of grouping. Hence, any difference between them can be attributed to the effect of the mutual constraint, which in this extreme case was such as to produce a common midspan deflection of all beams. Comparing the output strength CDF's of these two types for the same input population of beams shows to what extent a deck can enable stronger beams to help out weaker ones. Real beam and deck structures, of course, have a different kind of deck both in that it covers more of the beams and in that it is flexible. Real decks are thus in one sense better than, and in another sense not as good as, the single deck element of the prototype structure. Nevertheless, the analysis of this prototype should serve to provide some insight into the stochastic effects of a mutual constraint upon a system of beams. One should not expect any more than this from the analysis.

To compare brittlest-link and weakest-link structures, each type will next be analyzed.

## ***weakest - link structures***

“Weakest-link” structures are analogous to a chain in which every link carries an equal load; the chain fails when the load reaches the strength of the weakest link. Beam and deck structures with perfectly flexible deck are “weakest-link” because each member carries an equal share of the load.

At a given load per beam, increasing the number of beams increases the probability of failure by increasing the chances of getting a beam from the low

end of the strength range. This is the effect of grouping in weakest-link structures.

Let  $G_{in}$  = strength CDF of input population of beams,

$G_{out}$  = first break strength CDF of output population of structures,

and  $N$  = number of beams in structure.

By definition,  $G_{in}$  is the probability of failure of a single member. It is a function of  $P$ , the load on the member. Conversely  $1 - G_{in}$  is the probability of survival of a member. Similarly  $1 - G_{out}$  is probability of survival of a structure. But survival of a structure is simply the joint survival of  $N$  beams and since independent probabilities multiply, we get

$$1 - G_{out} = [1 - G_{in}]^N$$

or

$$G_{out} = 1 - [1 - G_{in}]^N \quad (2)$$

Equation (2) exhibits the effect of grouping in weakest-link structures. To see the effect of increasing  $N$  upon the strength of the structure, take  $G_{in}$  to be a so-called Weibull distribution (13):

$$G_{in}(P) = \begin{cases} 1 - e^{-\left(\frac{P-P_0}{\omega}\right)^m} & , P \geq P_0 \\ 0 & , P < P_0 \end{cases} \quad (3)$$

where  $P_0$  = lower limit of strength  $P$

$m, \omega$  = parameters chosen by fitting the distribution to experimental data

Substituting equation (3) into equation (2), the output CDF becomes

$$G_{out}(P) = 1 - e^{-N \left(\frac{P-P_0}{\omega}\right)^m} \quad , P \geq P_0 \quad (4)$$

Note that  $G_{out}$  equals  $G_{in}$  if  $N$  is unity. That is, one-beam structures are identically the same as the input population. The effect of increasing  $N$  is to

increase  $\bar{G}_{out}$  as shown graphically in figure 4 where  $P_0$ ,  $m$ , and  $N$  were fitted to the strength data of reference (6) for Grade 3 southern pine 2 by 8's. Note that at any given load, the probability of failure becomes greater as  $N$  is increased. The increasing steepness of the curve for larger  $N$  illustrates a decrease in variability. These are the characteristic effects of grouping (2, 12). Comparing input and output distributions, equations (3) and (4), it can be shown that the mean is reduced by the ratio

$$\frac{\bar{P}_{out} - P_0}{\bar{P}_{in} - P_0} = \left(\frac{1}{N}\right)^{1/m} \quad (5)$$

where  $\bar{P}_{out}$  = mean strength of output population

$\bar{P}_{in}$  = mean strength of input population

and the standard deviation is reduced by the same ratio:

$$\frac{\sigma_{out}}{\sigma_{in}} = \left(\frac{1}{N}\right)^{1/m} \quad (6)$$

where  $\sigma_{out}$  = standard deviation of output population

$\sigma_{in}$  = standard deviation of input population

Thus, the only stochastic effect present in weakest-link structures is one which reduces the apparent strength at all levels of probability except the very lowest. Since the safest design procedure is to assume that a structure is of the weakest-link type, it is clear that lumber grades must be characterized by their weakest pieces. The current practice is to assign allowable stresses which are near-minimum properties for the grade. The resulting low efficiency of the utilization led to the development of the load-sharing concept, and the hope of extracting some advantage from those structures which are not of the weakest-link type.

Next, for comparison, the results of an analysis of brittlest link structures are presented.

---

## ***brittlest - link structures***

---

A brittlest-link structure is by definition one in which the beam with the least deflection capacity fails first. The details of this analysis are presented in Appendix A. Since the output strength (first-break strength) CDF depends on both the stiffness and the deflection capacity of the input beams, the input population must be characterized by a bivariate CDF of two variables,  $k$  and  $\delta$ . Let

$G_{out}(P)$  = first-break strength CDF of output population of structures

$P$  = apparent strength. This has been defined as the total load on the structure divided by  $\underline{N}$

$k$  = stiffness of input beams

$\delta$  = deflection capacity of input beams

$F_{in}(k, \delta)$  = bivariate  $k$ - $\delta$  CDF of input beams

$H(\delta)$  = marginal  $\delta$  CDF of input beams, i.e.,  $H(\delta) = F_{in}(\infty, \delta)$

The derivative of a CDF is called the probability density function (PDF) and will be indicated hereafter by the use of lower case symbols. Thus,

$$f_{in}(k, \delta) = \frac{\partial^2 F_{in}(k, \delta)}{\partial k \partial \delta} = \text{bivariate } k\text{-}\delta \text{ PDF of input beams}$$

$$h(\delta) = \frac{dH(\delta)}{d\delta} = \text{marginal } \delta \text{ PDF of input beams}$$

Note that

$$h(\delta) = \int_{-\infty}^{\infty} f_{in}(k, \delta) dk \quad (7)$$

is a consequence of the preceding definitions.

In order to show the relation of  $G_{out}$  to  $F_{in}$ , some additional notation is required. Define

$$\left. \begin{aligned} p(k; \delta) &\equiv \frac{f_{in}(k, \delta)}{h(\delta)} \\ q(k; \delta) &\equiv \frac{\int_{\delta}^{\infty} f_{in}(k, \delta) d\delta}{\int_{\delta}^{\infty} h(\delta) d\delta} \end{aligned} \right\} \quad (8)$$

and let a star denote the operation of convolution:

$$p * q(t) = \int_{-\infty}^t p(x) q(t-x) dx \quad (9)$$

with repeated convolutions denoted by a star exponent:

$$q^{*N}(t) = q * q * \dots * q(t), \text{ N factors} \quad (10)$$

Then the output strength CDF of N-beam brittlest-link structures can be computed from the input bivariate PDF  $f_{in}(k, \delta)$  as follows (see Appendix A for derivation):

$$G_{out}(P) = \iint_{\underline{R}} \left[ 1 - H(\delta) \right]^{N-1} h(\delta) \cdot N p * q^{*(N-1)}(NK; \delta) d\delta dk \quad (11)$$

where  $\underline{R}$  is the region  $K\delta \leq P$ . This region is shown shaded in figure A2 in Appendix A. To evaluate equation (11), one must possess a function  $f_{in}(k, \delta)$  which has been fitted to experimental data for the input lumber grade and size. From  $f_{in}(k, \delta)$ , the functions  $p$ ,  $q$ ,  $H$ , and  $h$  are derived by equations (7) and (8) and substituted into equation (11), with convolutions formed according to equation (9).

#### The Uncorrelated Case

The labor of evaluating equation (11) is considerably shortened if the input population happens to have  $k$  and  $\delta$  uncorrelated. For the four cases to be studied below, the correlation coefficient between  $k$  and  $\delta$  is indeed small, in fact, less than 0.4. Whenever that is the case,  $f_{in}(k, \delta)$  can be closely fitted to the data by assuming a product form

$$f_{in}(k, \delta) = f_1(\delta) f_2(k) \quad (12)$$

for which the  $k$ - $\delta$  correlation coefficient is zero. Then, from equation (7),

$$h(\delta) \equiv f_1(\delta) \quad (13)$$

and, from equations (8),  $p$  and  $q$  reduce to

$$\begin{aligned} p(k; \delta) &= f_2(k) \\ q(k; \delta) &= f_2(k) \end{aligned} \quad (14)$$

that is,  $\underline{p}$  and  $\underline{q}$  are the same and are independent of  $\underline{\delta}$ . Thus, the convolutions in equation (11) reduce to

$$Np * q^{*(N-1)}(NK; \delta) = Nf_2^{*N}(NK) \quad (15)$$

Examination of data for four populations of low-grade lumber showed that the stiffness distribution is approximately normal in each case. This is indeed fortunate because it is known that the convolution of two normal PDF's is again a normal PDF whose mean is the sum of the means and whose variance is the sum of the variances. See reference (8). Thus, if  $f_2$  is chosen to be of normal form

$$f_2(k) = \frac{1}{\sigma\sqrt{2\pi}} e^{-1/2\left(\frac{k-\mu}{\sigma}\right)^2} \quad (16)$$

where  $\mu$  = mean of  $\underline{k}$

$\sigma$  = standard deviation of  $\underline{k}$  = square root of variance

then the  $\underline{N}$  convolutions in equation (15) simply increase the mean and variance by the factor  $\underline{N}$ . Thus:

$$\begin{aligned} Nf_2^{*N}(NK) &= \frac{N}{\sqrt{N\sigma^2}\sqrt{2\pi}} e^{-1/2\left(\frac{NK-N\mu}{\sqrt{N\sigma^2}}\right)^2} \\ &= \frac{\sqrt{N}}{\sigma\sqrt{2\pi}} e^{-N/2\left(\frac{K-\mu}{\sigma}\right)^2} \end{aligned} \quad (17)$$

Although the stiffness distribution is approximately normal, the distributions of strength and deflection capacity are ordinarily skewed to the left for low grade input populations. Thus, an exponential form is a better choice for  $f_1$  (i.e.,  $\underline{h}$ ). Accordingly, choose  $\underline{H}$  to be a Weibull distribution:

$$H(\delta) = \begin{cases} 1 - e^{-\left(\frac{\delta-\delta_0}{\omega}\right)^m} & , \delta \geq \delta_0 \\ 0 & , \delta \leq \delta_0 \end{cases} \quad (18)$$

where  $\delta_0$  = lower limit of  $\underline{\delta}$

$m, \omega$  = fitted parameters

Putting equations (17) and (18) into equation (11) yields the output CDF of

brittle-link structures for the uncorrelated case:

$$G_{\text{out}}(P) = \frac{N\sqrt{N} m}{\sigma\sqrt{2\pi} \omega} \int_{\delta_0}^{\infty} \int_{-\infty}^{P/\delta} \left( \frac{\delta - \delta_0}{\omega} \right)^{m-1} e^{-N \left( \frac{\delta - \delta_0}{\omega} \right)^m} e^{-N/2 \left( \frac{K-\mu}{\sigma} \right)^2} dK d\delta \quad (19)$$

By interchanging the order of integration, and introducing the change of variable

$$x = \left( \frac{P}{K} - \delta_0 \right) / \omega, \text{ equation (19) can be reduced to}$$

$$G_{\text{out}}(P) = Q \left( \frac{\frac{NP}{\delta_0} - N\mu}{\frac{\sqrt{N}}{\sigma}} \right) - \frac{P\omega\sqrt{N}}{\sigma\sqrt{2\pi}} \int_0^{\infty} e^{-N\phi(x)} \frac{dx}{(\omega x + \delta_0)^2} \quad (20)$$

where

$$\phi(x) = x^m + \frac{1}{2} \left[ \frac{\frac{P}{\omega x + \delta_0} - \mu}{\sigma} \right]^2$$

and

$$Q(t) = \frac{1}{\sqrt{2\pi}} \int_{-\infty}^t e^{-1/2t^2} dt = \text{Standard normal CDF}$$

The first term in equation (20) is the standard normal CDF or so-called “error function” and the second term can be integrated numerically.

Figures 5 through 8 show the application of this analysis to Grade 3 southern pine 2 by 8’s, using the data of reference (6). In figure 5, a normal CDF has been fitted to the data for stiffness, using MOE as a measure of  $\underline{k}$ . Figure 6 shows a

Weibull CDF fitted to data for deflection capacity  $\underline{\delta}$ , using  $\frac{\text{MOR}}{\text{MOE}}$  as a measure of  $\underline{\delta}$  (i.e., MOR is the measure of  $\underline{P}$ ). Since the correlation coefficient between  $\underline{\delta}$  and  $\underline{k}$  is only 0.0969 for this population, use of the simpler equation (20) in lieu of equation (11) is justified.

A simple test of validity is provided by setting  $N = 1$  in equation (20). The output strength CDF so generated should compare well with the strength data of the input population, since one-beam structures are identical to individual beams. Figure 7 shows the comparison and the agreement is seen to be good. This justifies the use of the uncorrelated model.

The effect of grouping in brittle-link structures is qualitatively similar to that effect in weakest-link structures. Figure 8 shows the input-output comparison for five-beam brittle-link structures, by plotting equation (20) for

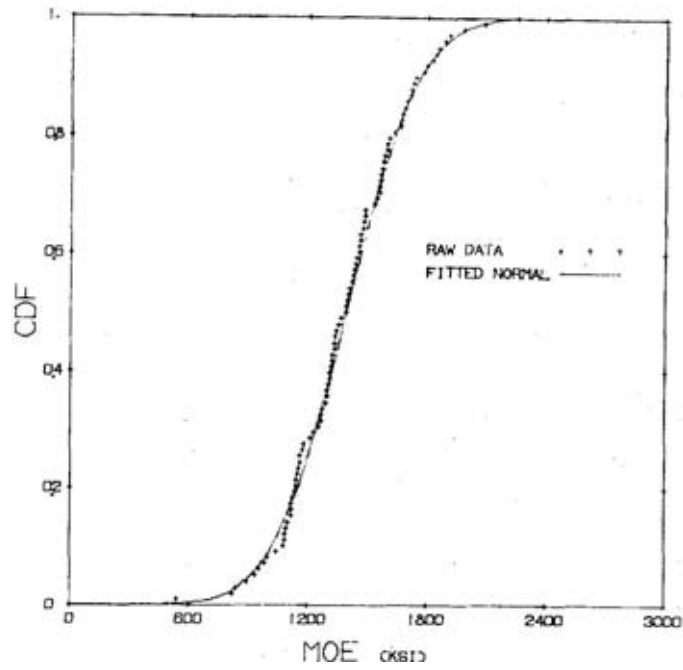


Figure 5.--Comparison of fitted normal distribution and raw stiffness data for Grade 3 southern pine 2 x 8's. M 136 648

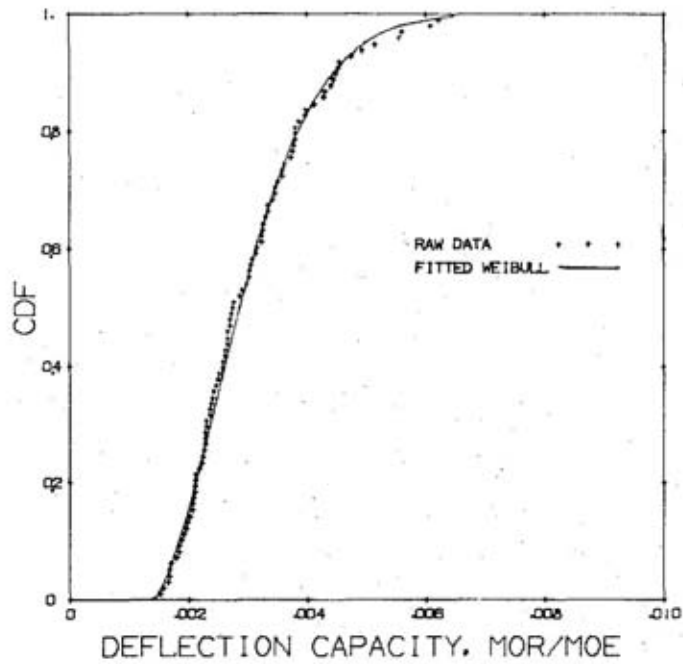


Figure 6.--Comparison of fitted Weibull distribution and raw data for deflection capacity of Grade 3 southern pine 2 x 8's.

M 136 651

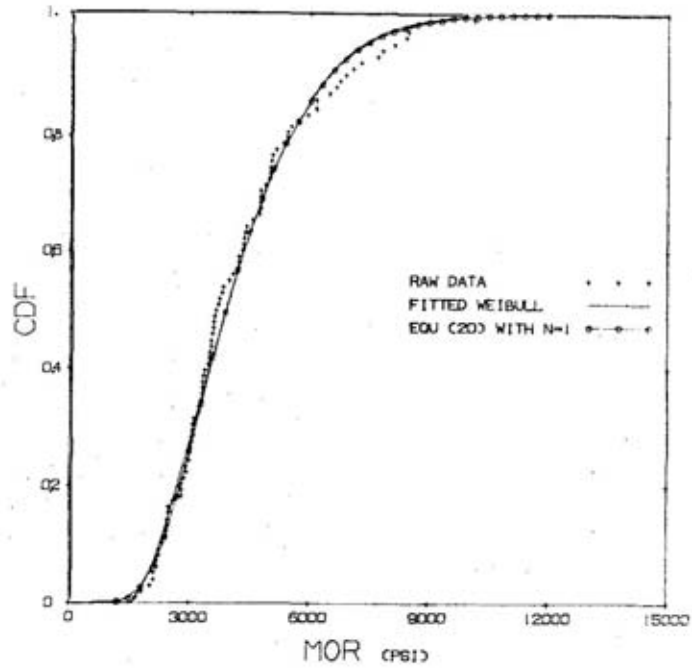


Figure 7. --Comparison of brittle-link algorithm, equation (20) at  $N=1$ , with raw strength data for Grade 3 southern pine 2 x 8's. Fitted Weibull distribution also shown. M 136 650

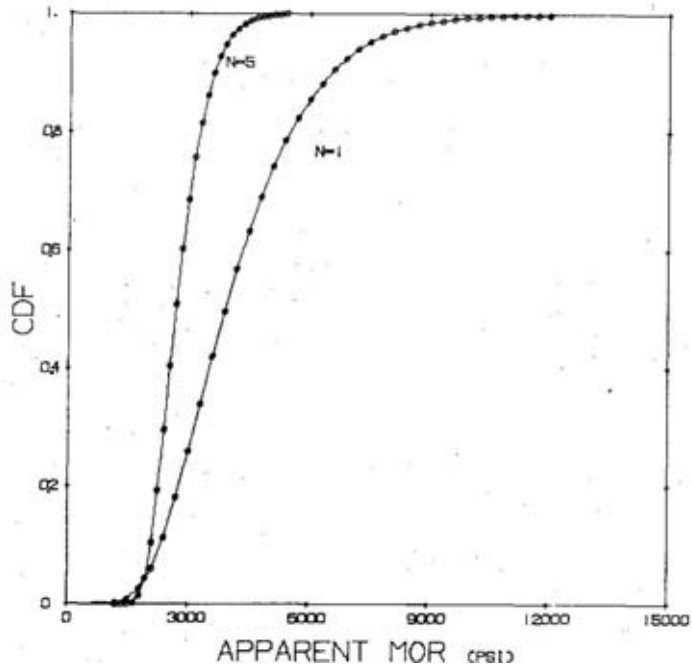


Figure 8.--Effect of grouping (size effect) in brittle-link structures. One-beam and five-beam structures of Grade 3 southern pine 2 x 8's compared for first-break capacity. M 136 649

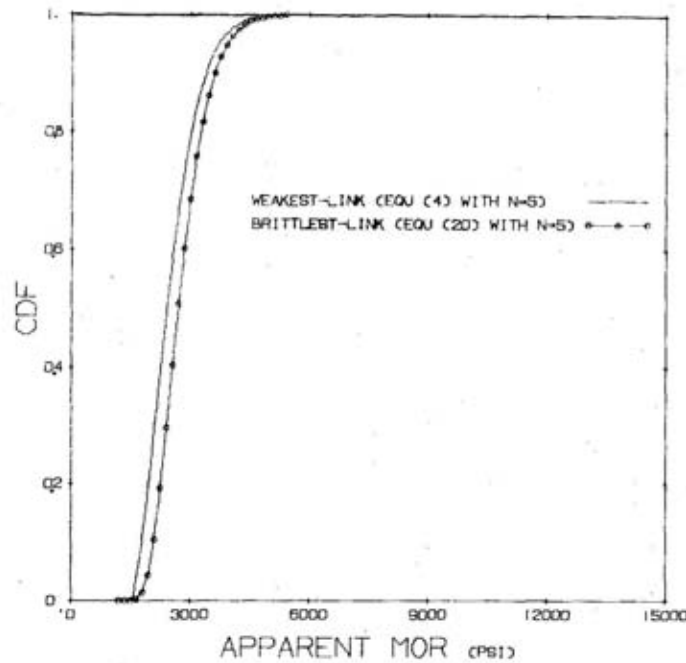


Figure 9.--Comparison of brittlest-link and weakest-link structures with N=5 beams of Grade 3 southern pine 2 x 8's. M 136 652

N = 1 and N = 5. The curve for N = 1 is the input strength distribution and the curve for N = 5 is the output. Comparison with figure 4 shows the similarity of the effect of grouping (or size effect) in the two types of structures. Note that the reduction in variability is identical for both types, but the depression of the mean is somewhat less for brittlest-link structures, indicating an effect of the mutual constraint.

To assess the effect of the constraint in brittlest-link structures without the distracting influence of grouping, a comparison with weakest-link structures of the same size must be made. Figure 9 compares five-beam structures of both types. Both are prototype structures with only a single deck element at midspan. The output CDF's are remarkably similar, the effect of the midspan constraint being a shift of about 250 p.s.i. to the right. That is, at all levels of probability the effect of the mutual constraint is to increase the apparent strength of this population by about 250 p.s.i. Such a simple uniform shift, however, is not necessarily typical, as will be seen below under "Application to Four Cases."

The strength of the input population at the 5 percent level is about 2,000 p.s.i. Using this as a base, the strength increase obtained from the mutual constraint is 12.8 percent. Giving the deck element a finite stiffness would reduce this, but extending the deck to cover the entire span would possibly increase it by local reinforcement of defects.

The effect of relaxing the stiffness of the deck element is investigated next.

## flexible deck structures

If the deck element of the prototype structure is neither infinitely rigid nor perfectly flexible, the analysis of load sharing due to mutual constraint is too complicated to be done in closed form. Here, a digital computer was used to simulate the testing of a large number of prototype structures with beams selected at random from a given input population and an approximate output CDF was generated by tabulating the results of 1,000 simulated tests.

Figure 10 shows a flow chart of the computer program. Raw test data were used as input; for each structure, five beams were selected at random with replacement; the weakest beam was always placed in the center position; the first-break failing load was computed from formulas that recognized the individual stiffness values of the beams and one-fifth the total load on the structure was converted to a modulus of rupture and recorded; the results of 1,000 such tests were tabulated into 100 strength classes; and finally, the output tabulations were accumulated and punched as the output strength CDF.

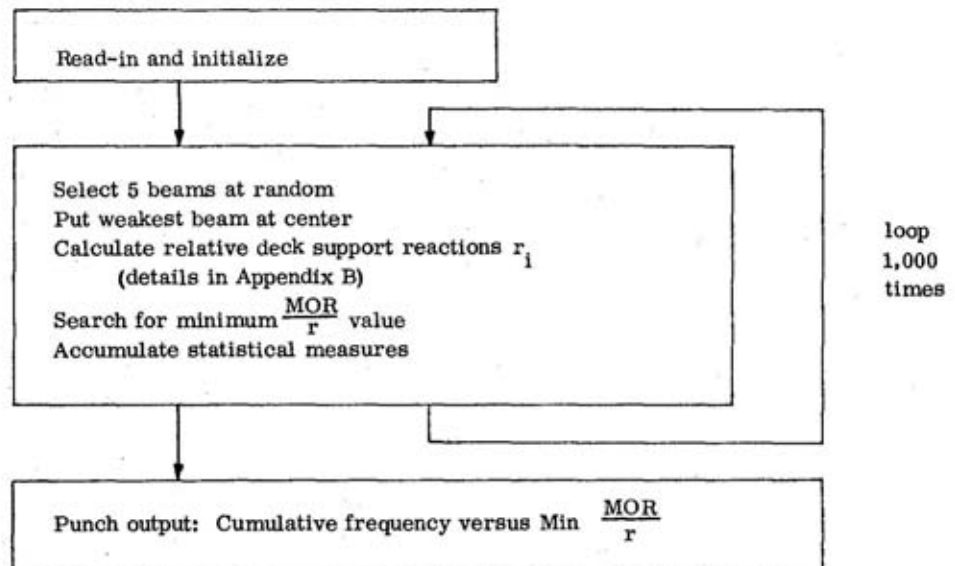


Figure 10.--Block diagram of computer simulation of structural tests.

Three values of deck stiffness were used with each input population, corresponding to  $\rho = 0.1, 1.,$  and  $10.,$  where

$$\rho = \frac{\text{Deck stiffness}}{\text{Modal value of stiffness of input beams}} \quad (21)$$

$$= \frac{(EI)_{\text{Deck}}}{(EI)_{\text{Beams}}} \cdot \left(\frac{L}{a}\right)^3$$

$L$  = beam span length,

$a$  = deck span length, i.e., beam spacing.

The modal value is the most frequently occurring one in a sample. It corresponds to the maximum of the PDF, The computer algorithm for getting the apparent MOR of a structure with five dissimilar beams is derived and presented in Appendix B. The results of the computer simulation approach are shown in the next section.

---

## ***application to four cases***

---

The need for bivariate characterization imposes severe sample size requirements on the input population in both the computer simulation approach and the brittlest-link analysis. Furthermore, since the effect of grouping is to compress the strength distribution toward its lower limit, the low extremes of the distributions must be well established. These requirements made it difficult to find suitable input data for this study. Four fairly large samples were available: Two of size 98 (6) and two of size 80 (7). These are not large enough to show reliable behavior in the low extremes, however, and some educated guesswork was needed to establish lower limits of strength and deflection capacity. If this estimation is done in a consistent fashion, however, the error in the effect of grouping should be similar for both weakest-link and brittlest-link analyses, and hence their comparison should yield a useful measure of the effect of a mutual constraint in spite of some uncertainties about the low extremes. Table 2 shows the four sets of data used as input populations. Hereafter they will be referred to by case number as shown in the table.

In each case the first step was to fit mathematical distribution functions to the data. The Weibull-type exponential CDF (see eq. (3)) was fitted to the strength data with MOR as the measure of strength  $\underline{P}$ , the same form CDF (eq. (18)) was fitted to deflection capacity data using the ratio MOR/MOE as the measure of deflection capacity  $\underline{\delta}$ , and the Gaussian normal PDF (eq. (16)) was fitted to the stiffness data with MOE as the measure of stiffness  $\underline{k}$ . The normal curve was fitted by the usual method of moments; the Weibull curve was fitted by least squares in a transformed plane as described in Appendix C. Table 3 summarizes the results of the curve fitting. Since a normal curve was fitted to MOE, it is important that the stiffness data not be skewed; the table shows both the mode and the mean as an aid in assessing skewness. Only cases 1 and 2 were moderately skewed. Note that case 3 was fitted two ways for comparison; these will be referred to hereafter as cases 3a and 3b. In every case but 3b, the lower limits of strength and deflection capacity distributions were taken to be 90 percent of the smallest sample value; in case 3b the lower limits were set to zero, resulting in poorer fits and a smaller load sharing effect.

Table 2.--The four input populations

Case	Species	Grade	Size	Sample size	Source of Data
1	Southern pine	3	2 by 8	98	(6)
2	Southern pine	3	2 by 4	98	(6)
3	Douglas-fir	Construction	2 by 4	80	(7)
4	Douglas-fir	Standard	2 by 4	80	(7)

Table 3.--Summary of fitted parameters'

Variable	Case	Lower limit		m	w	Mode	Mean, $\mu$	Standard deviation, $\sigma$	k - $\delta$ correlation
		$P_0$	$\delta_0$						
		P.s.i.	P.s.i.	P.s.i.	K.s.i.	K.s.i.	K.s.i.		
P:MOR	1	1,510		1.645	3,005				
k:MOE						1,200	1,392	290.5	0.0969
$\delta$ :MOR/MOE			0.001362	1.668	0.001867				
P:MOR	2	2,080		1.560	3,855				
k:MOE						1,300	1,375	387	-0.177
$\delta$ :MOR/MOE			.001666	1.770	0.002749				
P:MOR	3a	1,910		2.194	6,063				
k:MOE						2,066	2,066	378	-0.0266
$\delta$ :MOR/MOE			.00119	2.500	0.002551				
P:MOR	3b	0		3.161	8,364				
k:MOE						2,066	2,066	378	-0.0266
$\delta$ :MOR/MOE			0.00000	3.816	0.003786				
P:MOR	4	1,385		1.564	4,050				
k:MOE						1,750	1,751	363	.356
$\delta$ :MOR/MOE			.000879	2.325	0.002149				

<sup>1</sup>Values of mode and correlation coefficient are not fitted parameters, but are population measures, and are shown for information.

Scatter diagrams of  $k$  vs.  $\delta$  are shown in figure 11. Even though the  $k - \delta$  correlation coefficient is rather high for case 4, all four cases were treated as uncorrelated in analyzing their brittlest-link behavior. Some measure of the errors due to this assumption and to small sample size can be seen by comparing the output strength CDF of one-beam brittlest-link structures from equation (20) with the raw strength data, as was done previously for case 1 in figure 7. If  $N = 1$ , equation (20) reduces to an algorithm for generating the strength distribution of a population of beams from its stiffness and deflection capacity distributions. This "N = 1 test" is shown in figures 12, 13, 14, and 15, for cases 2, 3a, 3b, and 4, respectively.

Figures 16 to 20 show output CDF's of weakest-link five-beam structures and brittlest-link five-beam structures as smooth lines, and include for comparison the output CDF's generated by the computer simulation approach. These appear as jagged lines since the input data were not smoothed by curve fitting for the flexible deck structures. These curves lie more or less between the smooth curves for zero deck stiffness and infinite deck stiffness except for irregularities associated with the small sample size of the input and the lack of any smoothing. Thus, as might be expected, the limiting cases analyzed in closed form appear to be upper and lower bounds on the output CDF's obtainable with a flexible deck element.

Table 4 shows a summary of the load-sharing effect due to a mutual constraint in the prototype structure of this study. The "load-sharing increase" (LSI) shown in the table is the difference in strength between brittlest-link and weakest-link five-beam structures expressed as a percent of the strength of the input population, with all strength values measured at the 5 percent level, i.e., where the strength CDF equals 0.05. Thus by definition

$$LSI \equiv \frac{P_{out} | G_{out} = .05 - P_{in} | G_{in} = .05}{P_{in} | G_{in} = .05} \quad (22)$$

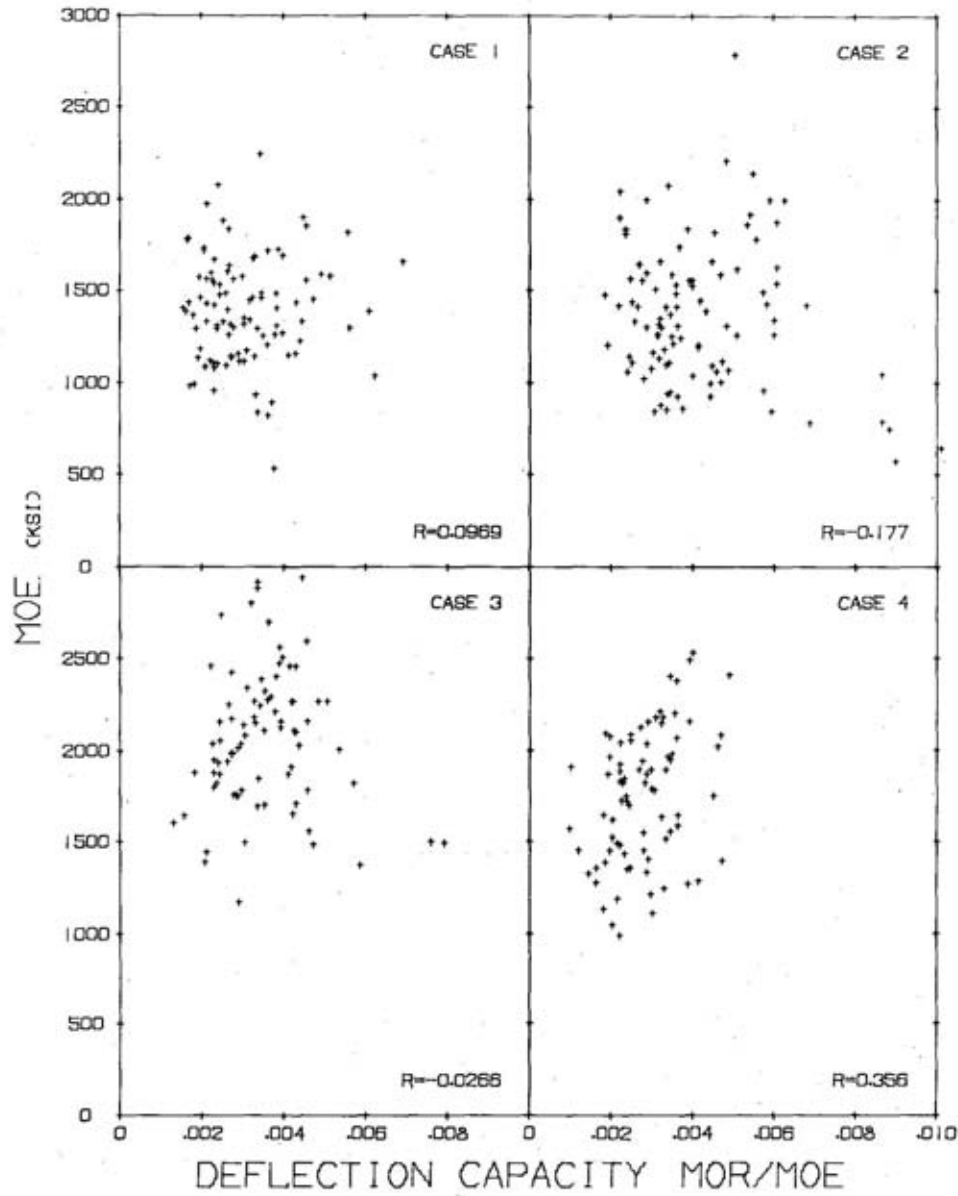


Figure 11.--Scatter diagrams of stiffness versus deflection capacity for the four cases studied. Correlation coefficients shown on the diagrams.

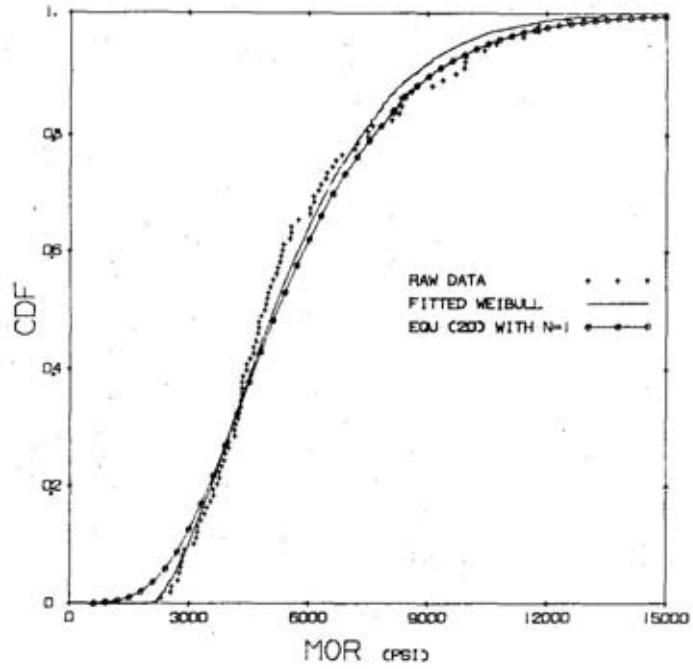


Figure 12.--Comparison of brittlest-link algorithm equation (20) at  $N=1$  with raw data for case 2. Fitted Weibull distribution also shown. M 136 653

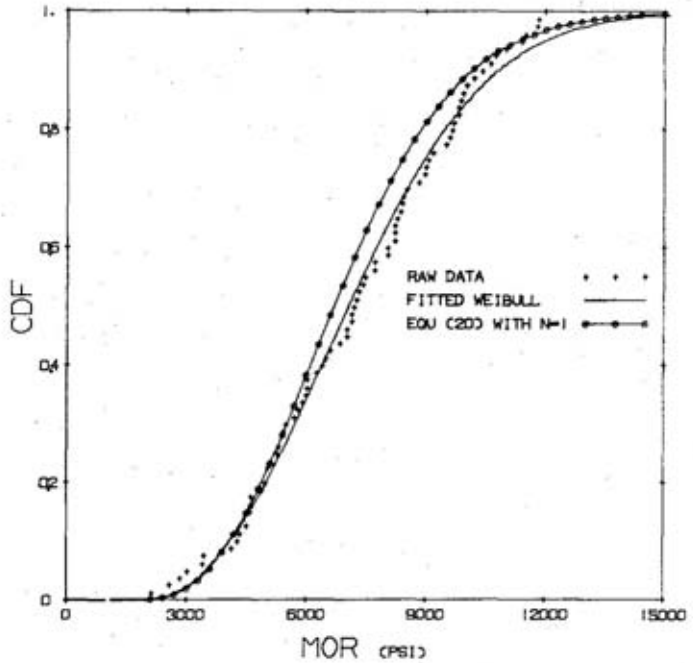


Figure 13.--Comparison of brittlest-link algorithm equation (20) at  $N=1$  with raw strength data for case 3a. Fitted Weibull distribution also shown, with  $P_0$  chosen to make low tails conform. M 136 647

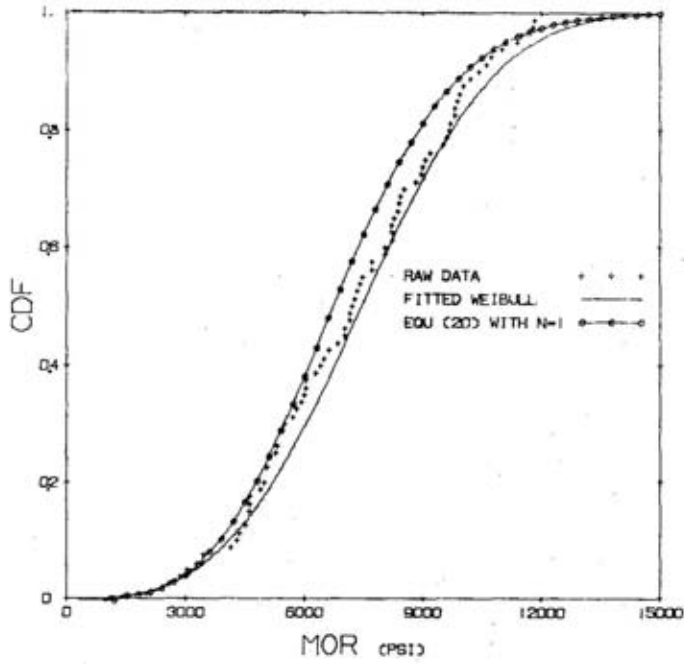


Figure 14.--Comparison of brittlest-link algorithm equation (20) at  $N=1$  with raw strength data for case 3b. Fitted Weibull distribution also shown, with  $P_0$  chosen to make low tails conform. M 136 637

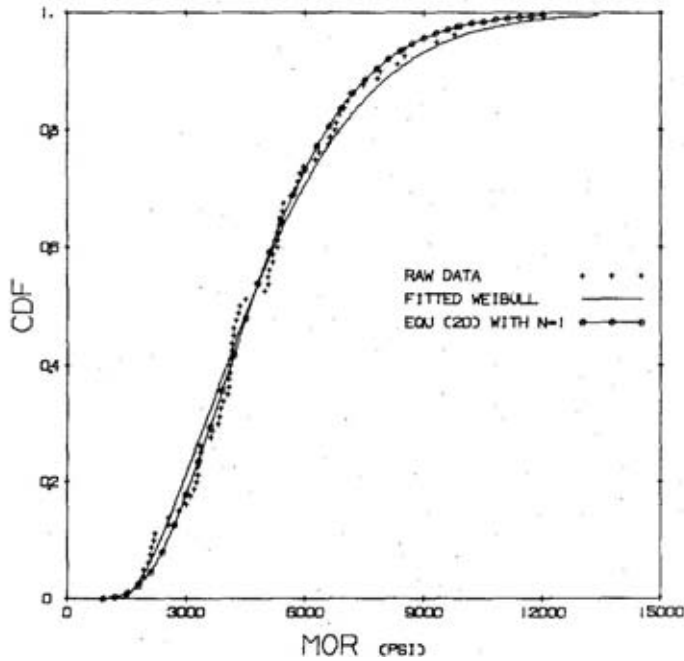


Figure 15.--Comparison of brittlest-link algorithm equation (20) at  $N=1$  with raw strength data for case 4. Fitted Weibull distribution also shown. M 136 636

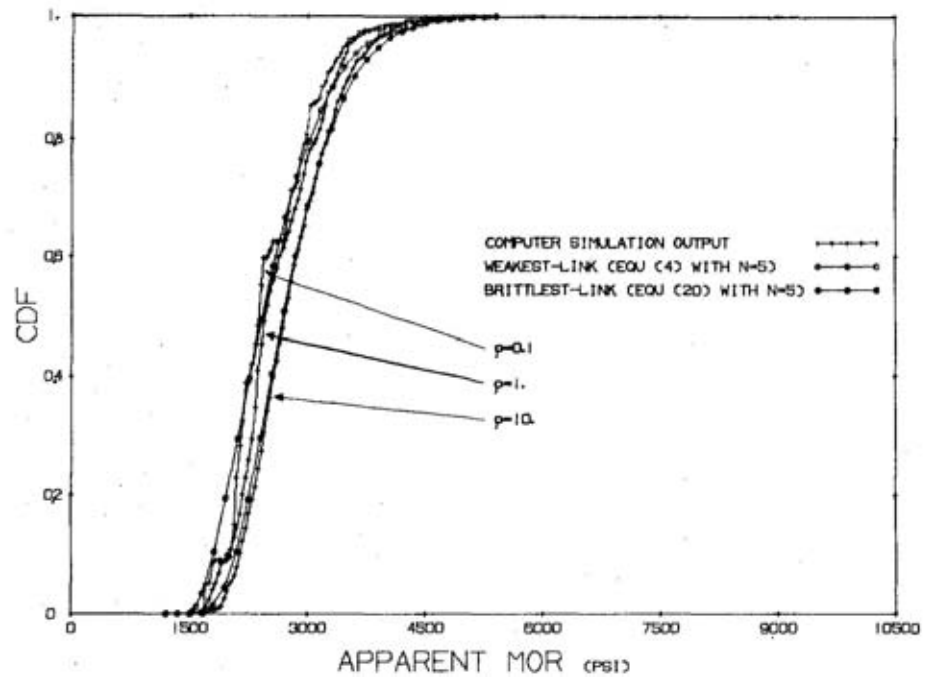


Figure 16.--Effect of deck stiffness on capacity of five-beam structures. Equations (4) and (20) are compared as in figure 9, and computer simulation output is superimposed for comparison. Case 1.

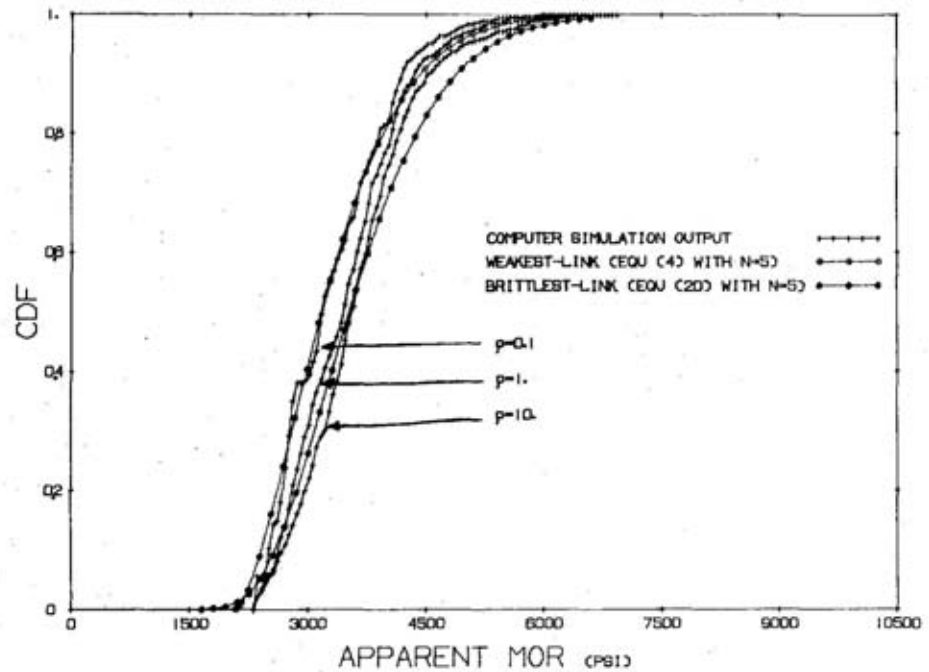


Figure 17.--Effect of deck stiffness on load capacity of five-beam structures. Equations (4) and (20) and computer simulation output are compared for case 2.

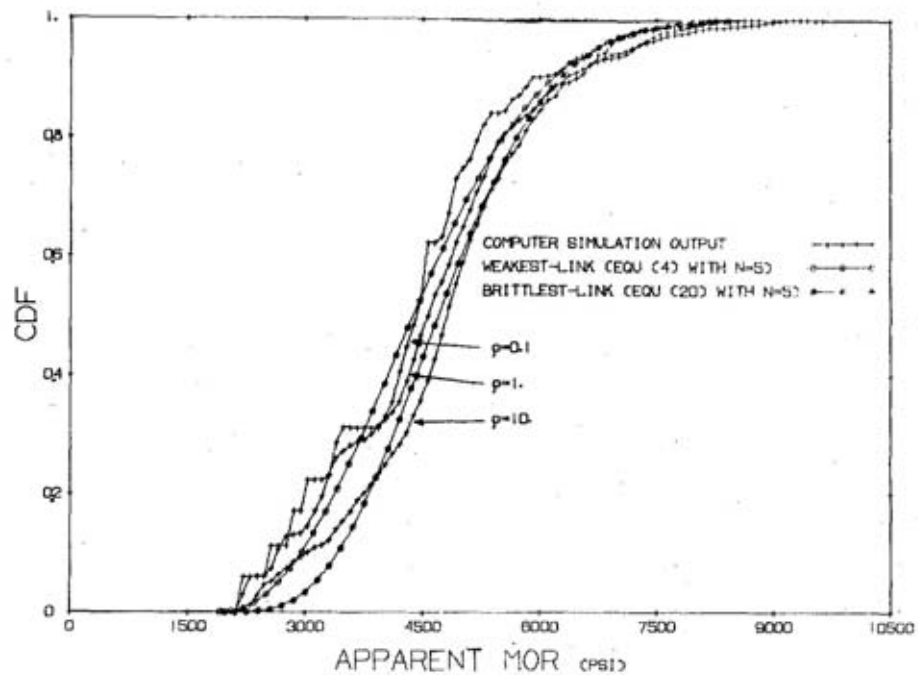


Figure 18.--Effect of deck stiffness on capacity of five-beam structures. Equations (4) and (20) and computer simulation output compared for case 3a.

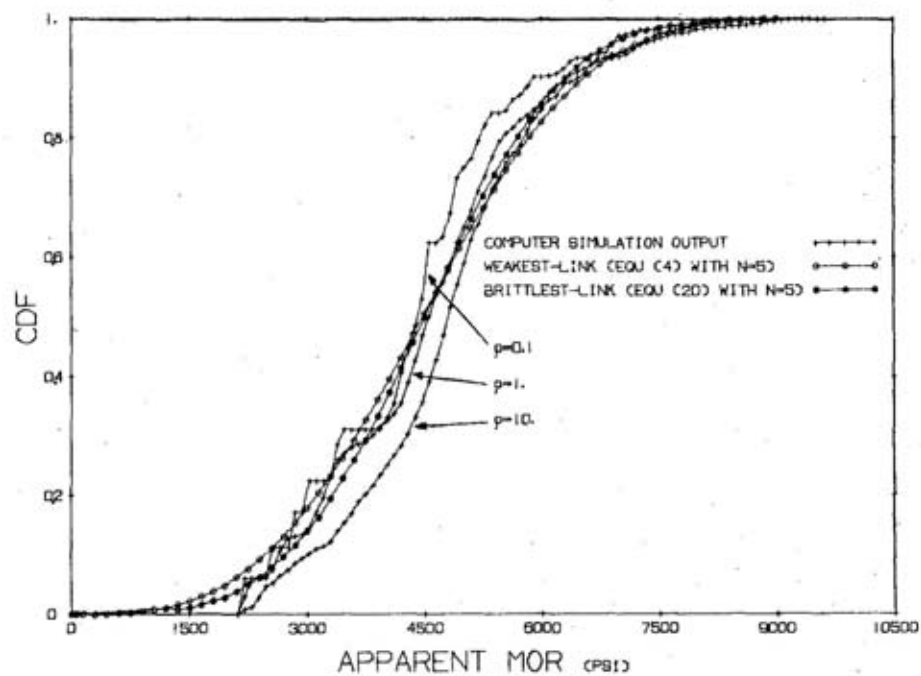


Figure 19.--Effect of deck stiffness on capacity of five-beam structures. Equations (4) and (20) and computer simulation output are compared for case 3b.

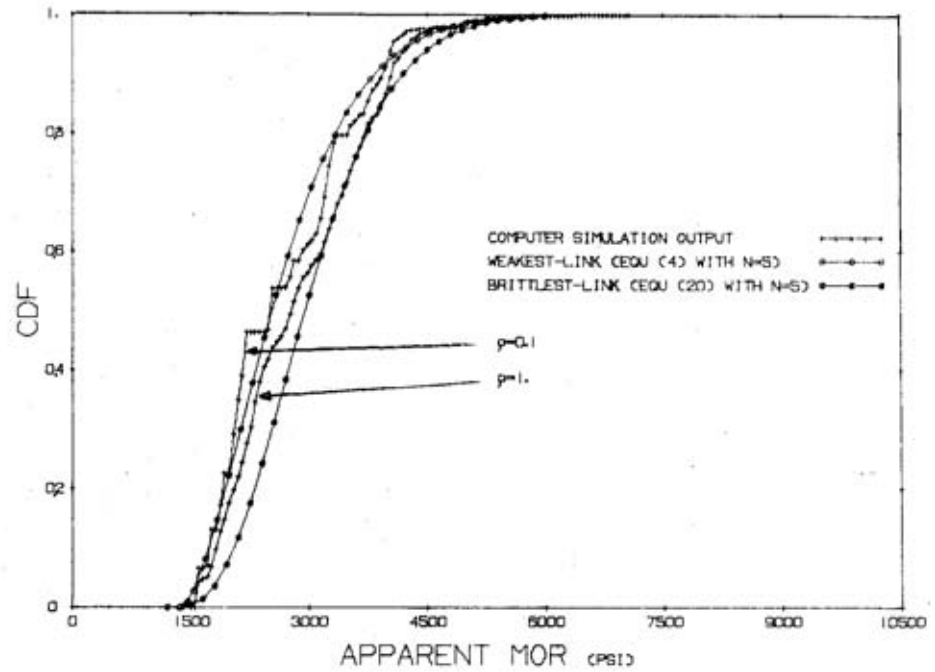


Figure 20.--Effect of deck stiffness on capacity of five beam structures. Equations (4) and (20) and computer simulation output are compared for case 4.

Table 4. --Summary of load-sharing effects

Case	Strength at 5 percent level (exceeded by 95 pct. of population)			Load sharing increase (LSI)
	five-beam weakest-link structures <sup>1</sup>	five-beam brittlest-link structures <sup>2</sup>	input population <sup>3</sup>	col (3) - col (2)
(1)	(2)	(3)	(4)	(5)
				<u>Pct.</u>
1	1,703	1,960	2,005	12.8
2	42,605	42,860	2,655	9.6
3a	2,660	3,095	3,475	12.5
3b	1,960	2,228	3,270	8.2
4	1,600	1,850	1,992	12.5

<sup>1</sup>Equation (4) with N = 5

<sup>2</sup>Equation (20) with N = 5

<sup>3</sup>Equation (3) with N = 5

<sup>4</sup>At 20 pct. level. See discussion of case 2.

Each case will now be discussed separately.

Case 1.--In this case, all the assumptions of the theory are well met by the data. There is little skewness or deviation from normalcy in the stiffness distribution. The strength distribution is smooth and well fitted by the Weibull exponential form (eq. (3)) as can be seen in figure 7. The correlation coefficient of  $\underline{k}$  and  $\underline{\delta}$  is only 0.0969, which is not significantly different from zero. Furthermore the scatter diagram of  $\underline{k}$  versus  $\underline{\delta}$  (figure 11) shows that the product form of bivariate distribution (eq. (12)) may be expected to fit these data extremely well, and the close agreement of brittlest-link and weakest-link theories at  $N = 1$  in figure 7 bears this out. It is not surprising, therefore, that the computer simulation output agrees well with the theoretical curves at  $N = 5$  as shown in figure 16. Note, too, how the computer simulation output is smoother when the deck is stiffer--an indication that irregularities due to sampling error tend to smooth out under the influence of the mutual constraint. The computed LSI for this case is 12.8 percent.

Case 2.--Here the assumptions of the theory are not met as well as in case 1. The negative correlation between  $\underline{k}$  and  $\underline{\delta}$  means that low  $\underline{\delta}$  implies high  $\underline{k}$  and vice versa. But the theoretical model is uncorrelated, so it contains some low  $\underline{k}$  - low  $\underline{\delta}$  members which are not present in the real sample; figure 12 shows the results of this. The  $N=1$  test of brittlest-link theory has a fat low tail; these are the low  $\underline{k}$  - low  $\underline{\delta}$  (and hence low  $\underline{k\delta}$  or low strength) members which are present in the theory but not in the raw data. Despite this difficulty, the overall fit in figure 12 is fairly good. The comparison at  $N = 5$  in figure 17 also shows reasonable agreement between theory and numerical experiment with the exception of the poor showing of brittlest-link theory in the extremes of the distribution. The low tail of the brittlest-link distribution at  $N = 5$  is too heavy and continues to cross over the weakest-link curve as it did at  $N = 1$  and hence one cannot reasonably compute an LSI at the 5 percent level for this case. Instead, the 20 percent level was used to calculate the strength increment of five-beam structures and this was expressed as a percent of the input strength at the 5 percent level. The LSI computed by this modified definition is 9.6 percent. Note however that the computer simulation output does not show much effect of the constraint in the low tail of the output distributions for this case.

Case 3a.--Here the data were fitted in a manner consistent with cases 1, 2, and 4. The correlation coefficient between  $\underline{k}$  and  $\underline{\delta}$  is only -0.0266. Thanks to this low value, the brittlest-link algorithm passes the  $N = 1$  test fairly well (fig. 13) considering the irregular scatter of these data. Note that equations (4) and (20) agree especially well in the low tail. This is important to the accurate computation of the LSI. At  $N = 5$ , the comparison in figure 18 shows a 12.5 percent LSI and the computer simulation output again confirms the general trend of the theoretical curves despite the irregularities in this somewhat smaller sample.

Case 3b.--This case used the same input population as case 3a, but the data were fitted in an alternate manner: The lower limits of strength and deflection were taken to be zero. This appears to do an adequate job of fitting at  $N = 1$  according to figures 14 and C2. The  $N = 1$  test does not look quite as good as case 3a, however (compare figs. 13 and 14), and the comparison at  $N = 5$  shows very poor agreement between brittlest-link theory and computer simulation output at  $\rho = 10$ . Furthermore, figure 19 reveals that weakest-link and brittlest-link models nearly agree at  $N = 5$ , whereas they should have agreed at  $N = 1$ .

This experiment reveals the importance of the parameters  $\underline{P}_0$  and  $\underline{\delta}_0$ , and indicates that they must be chosen realistically, not conservatively. The LSI value of 8.2 percent is probably not as meaningful as the value computed in case 3a.

Case 4.--The results for this case are surprisingly good in view of the rather large correlation of 0.3558 between  $\underline{k}$  and  $\underline{\delta}$ . Figure 15 shows that the brittlest-link algorithm satisfies the  $N = 1$  test extremely well despite its assumption that  $\underline{k}$  and  $\underline{\delta}$  are uncorrelated. Since case 2 produced such poor results with a  $\underline{k} - \underline{\delta}$  correlation of  $-0.177$  and since case 1 fared better than case 3 even though the correlation was larger in case 1, one is led to conjecture that the sign of the correlation between  $\underline{k}$  and  $\underline{\delta}$  may be more important than its magnitude. Good results were obtained whenever the correlation was positive. Figure 20 shows that the agreement with the computer simulation at  $N = 5$  is also excellent. The LSI for this case is 12.5 percent.

---

## ***discussion***

---

The main objective of the present paper is to offer insight into the probable magnitude of the load-sharing effect due to a mutual constraint. A one-dimensional deck element is sufficient for this purpose. The results presented in table 4 indicate that the effect is not great, although it certainly does exist. The increase of only about 12 percent is neither confirmed nor denied by the experimental results of other investigators to be discussed below. A small outcome is, however, believable when one looks at a typical scatter diagram of strength versus deflection capacity such as figure 21. Load sharing will increase load capacity only if the weaker members possess sufficient deflection capacity to deflect out of the way without failing. But figure 21 shows that strength and deflection capacity tend to correlate well. Hence only a small minority of weak members have the necessary deflection capacity to survive in a brittlest-link structure, and it is only from these few that a meager load-sharing increase can be obtained.

But is the ratio of MOR to MOE a true measure of deflection capacity? That is, do individual beams behave in a linear elastic fashion all the way to failure? Surely not all of them do, but the weaker ones are presumed to do so. That is why all load-sharing comparisons were made at the 5 percent level in table 4. Behavior at the high end of the distribution should not be regarded as realistic: neither is it of much interest. Floor tests at the Oregon State University Forest Research Laboratory have confirmed the assumption that the system behaves in a linear elastic manner until first break (1). They also show that the nonlinear behavior beyond first break contributes significantly to the ultimate load capacity of the system. Because of the close relationship of this experimental work to the present study, it will be discussed next in more detail.

The effect of nailing 1/2-inch sheathing-grade plywood to a simply supported system of beams under uniform load has been extensively studied at Oregon State University's Forest Research Laboratory. Their tests of 14-beam structures showed that the first-break load of utility-grade Douglas-fir 2 by 6's was increased about 45 percent by the addition of the plywood deck. Other grades and sizes showed increases of only 7 to 30 percent. Ultimate load capacity was found to be about 1-1/2 times as great as first-break load. Table 5 shows the grades

and sizes tested and gives the increase in load capacity as a percent of the load capacity of floor systems without decks. Ninety-five percent confidence limits are shown in parentheses. Results on eachline are obtained from averages of five floor tests. Thus sample means are compared here whereas LSI was defined in terms of a comparison at the 5 percent level. Comparison of means was necessitated by the small sample size, which prevents any reliable estimation of the 5 percent exclusion limit. Load capacity of the floor systems without decks was obtained from individual tests of matched beams, taking the least MOR of a group of 14 as the load capacity of a "floor without deck."

The rather large confidence intervals shown in table 5 are the result of small sample size and indicate that five structures do not tell much about the population of possible structures obtainable from the given beams. This is the inherent weakness of an experimental approach to the load-sharing problem. In spite of the inconclusive nature of these data, however, they do seem to imply that the strength of the structure is likely to be greater than what this simplified theoretical analysis is able to account for. The extra increase is probably due to the mechanical effect of T-beam action and the third stochastic effect listed in the Introduction, namely that due to local reinforcement of defects. These two effects will be considered next in more detail.

Table 5.--Increase in load capacity of floors due to addition of 1/2-inch plywood deck

Grade	Species	Size	Percent increase due to deck <sup>1</sup>		Span
			First break	Ultimate	
Utility	Douglas-fir	2 by 6	45 (16 to 75)	168 (126 to 211)	9 ft.
Utility	Western hemlock	2 by 10	18 (-30 to 66)	80 (48 to 112)	15 ft. 4 in.
Utility	Douglas-fir	2 by 10	30 (-25 to 86)	117 (81 to 153)	15 ft. 4 in.
Standard or better	Douglas-fir	2 by 10	7 (-55 to 68)	86 (43 to 130)	17 ft. 1 in.

<sup>1</sup>First number is average of 5 floor tests; 95 percent confidence limits are shown in parentheses.

### T-Beam Action

To estimate the influence of T-beam action upon first-break load, a linear theory of nailed composite beams may be used. Treating each beam as a T-beam with a 16-inch-wide flange of 1/2-inch plywood joined by an eightpenny nail every 10 inches, the theory of reference (9) predicts an increase in effective section modulus of 11 percent for the 2 by 6 joists, 7.2 percent for 2 by 10 joists on a 15-foot 4-inch span, and 3.2 percent for 2 by 10 joists on a 17-foot 1-inch span. Since the strength increases shown in table 5 are considerably greater than this, it is evident that these data confirm the existence of some effect due to mutual constraint and local reinforcement of defects.

### Local Reinforcement of Defects

The effect of local reinforcement of defects was not theoretically modeled in this study but is present in the experimental results cited above. Since plywood decks can sustain two-dimensional solid-membrane stresses, it is evident that they can bridge local defects. Whereas plywood sheets are easily bent into singly curved or developable surfaces, they strongly resist double curvature because of the membrane stresses that accompany such deformation; hence, an isolated local defect may be effectively stiffened by this two-dimensional action which also transfers some load away from the defective point. Thus, the low local stiffness in the immediate neighborhood of a defect may be more important to load sharing than the slightly lower  $k$  value of the member as seen in a bending test, if the deck material is of sheet form such as plywood. To model this local reinforcement effect theoretically would raise the input information requirement by an order of magnitude, since variability within members would have to be specified in addition to the variability among members. The prospect seems of doubtful value. The two-dimensional redistribution of load in the neighborhood of a local defect could be studied in a single well-instrumented test, however, without regard to its stochastic implications.

---

## **summary**

---

The load-sharing concept asserts that wood beam and deck structures are not of the weakest-link type and their design need not be based on the strength of the weakest member. This report analyzed brittlest-link structures and compared them with the weakest-link type. A simple prototype structure was employed.

Composite action of the deck (T-beam action) was not studied; instead an effect was sought which was independent of the strength of the deck or the stiffness of its fasteners. In the analysis, the deck is present only as a constraint on the deflections of the beams. Its structural contribution to the system was ignored, as it is in design. Only the stochastic effect of a mutual constraint upon the load performance of the system was sought.

The analysis of brittlest-link structures was based on two fundamental assumptions:

1. Linear load-deflection relationship for each beam.
2. Load capacity of a structure is determined by the load at which the first beam breaks.

The first assumption is reasonable for low-grade lumber and is supported by experimental evidence (Oregon State University) up to the load at which first break occurs. The second assumption was necessitated by considerations of mathematical convenience. Research at Oregon State suggests that the ultimate load is at least about 1.5 times the first-break load. If failure is defined in terms of user satisfaction however, first-break load seems to be a reasonable definition.

Assembly of beams into structures entails three stochastic effects derived

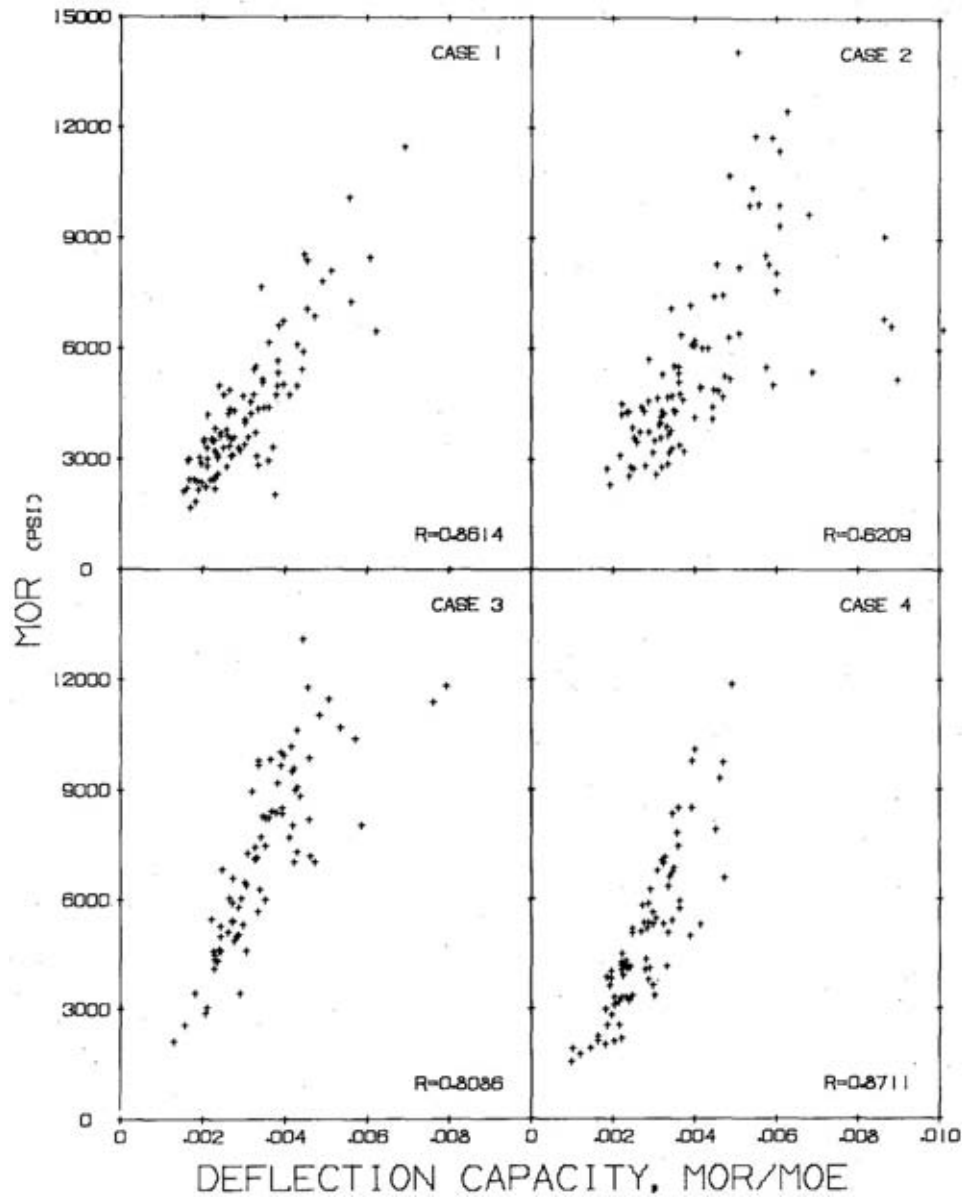


Figure 21.--Scatter diagrams of strength versus deflection capacity for the four cases studied. Correlation coefficients shown on the diagrams.

from the variability in mechanical properties of wood beams. They are:

1. Grouping (size effect)
2. Mutual constraint
3. Local reinforcement of defects

Effects (1) and (2) tend to reduce the apparent variability among members; effect (3) reduces the apparent variability within members and was not studied.

What is called "grouping" here is essentially size effect in structures. It is qualitatively similar to the size effect that has been noted in individual members.

It is characterized by a reduction in variability and a decrease in mean strength such that the minimum strength stays the same. "Mutual constraint"--provided by a deck element--shifts the nature of the structure from equal beam loads to equal beam deflections. This affects the first-break load by changing the mode of failure from weakest link to brittlest link. This shift does not alter the reduction in variability since strength and deflection capacity of wood beams happen to be about equally variable, but it does affect the minimum strength. The 5 percent exclusion limit was used as the index of minimum strength since it can be more reliably estimated than minimum strength.

Using data on strength and stiffness for four populations of wood beams, the increase in minimum load capacity from effect (2) was computed for each case. The results, summarized in table 4, indicate a load-sharing increase of about 12 percent. This is too high because real decks are not rigid enough to impose equal deflections, and too low because effect (3) was not included. It is vitally dependent upon the particular strength and stiffness distributions of the beam population and could be greater or less depending upon the size, grade, and species of the beams.

---

### ***literature cited***

---

- (1) Atherton, G. H., and Corder, S. E.  
1965. Strength of floors with 2 by 6 Douglas-fir utility-grade joists. Preliminary Rep., Forest Res. Lab., Oreg. State Univ., Corvallis.
- (2) Bohannon, B.  
1966. Effect of size on the bending strength of wood members, U.S. Forest Serv. Res. Pap. FPL 56, Forest Products Lab., Madison, Wis.
- (3) Bonnicksen, L. W.  
1964. Structural reliability of some equally deflected multibeam systems. ASAE Pap. No. 64-407, Amer. Soc. Agr. Eng., St. Joseph, Mich.
- (4) \_\_\_\_\_  
1965. Structural reliability of vertically laminated wood beams. Ph. D. thesis, Purdue Univ.
- (5) \_\_\_\_\_ and Suddarth, S. K.  
1966. Structural reliability analysis of a wood load-sharing system, J. Mater., Vol. 1, No. 3, p. 491.
- (6) Doyle, D. V., and Markwardt, L. J.  
1966. Properties of southern pine in relation to strength grading of dimension lumber. U.S. Forest Serv. Res. Pap. FPL 64, Forest Prod. Lab., Madison, Wis.
- (7) Johnson, J. W.  
1960. Random products method to set stresses for lumber. Supplement to Rep. T-20, Forest Res. Lab., Oreg. State Univ., Corvallis.

- (8) Kendall, M. G., and Stuart, A.  
1958. The advanced theory of statistics. Vol. 1, Distribution theory. Hafner Publ. Co., New York, p. 192.
- (9) Mohler, K.  
1956. Über das Tragverhalten von Biegeträgern und Druckstäben mit zusammengesetzten Querschnitten und nachgiebigen Verbindungsmitteln. (On the behavior of built-up beams and columns with nonrigid connectors.) Ph.D. thesis, Technischen Hochschule Fridericiana zu Karlsruhe, Deutsch.
- (10) National Association of Home Builders  
1961. The effect of framing and subfloor attachment on the stiffness of residential floors. Res. Inst. Lab.
- (11) Russell, W. A.  
1954. Deflection characteristics of wood floor systems, Housing and Home Finance Agency, Housing Res. Pap. No. 30.
- (12) Weibull, W.  
1939. A statistical theory of the strength of materials, Swedish Royal Inst. Eng. Res. Proc., Stockholm
- (13) \_\_\_\_\_  
1951. A statistical distribution function of wide applicability. J. Appl. Mech. 18: 293-297.
- (14) Williston, E. M., and Abner, T. L.  
1962. Design criteria for wood floor systems. Forest Products J. 12(9): 403-409.
-

---

## appendix A

---

### Strength of Brittle-Link Structures

The output strength CDF of N-beam brittlest-link structures is derived here. The result is quoted in the body of the report as equation (11). Notation not defined here has been defined in the body of the report.

For simplicity, a three-beam structure will be illustrated and generalized to N beams at a convenient point in the derivation. Figure A1 shows typical load-deflection diagrams for three beams. They are assumed to be linear to failure. Let these three beams be assembled into a prototype structure with a rigid deck element. Assume the deck is so loaded as to remain horizontal. First break will be taken as the criterion of structural failure. Then, since all beams are constrained to have the same center deflection, the deflection at failure will equal the deflection capacity of the brittlest beam. Call this beam No. 1, and number the others in any order. Since each beam carries a force in proportion to its stiffness, the total load on the structure is (see fig. A1):

$$Q = k_1 \delta_1 + k_2 \delta_1 + k_3 \delta_1 = (k_1 + k_2 + k_3) \delta_1 \quad (A1)$$

and the apparent strength of each of the three beams is

$$P = \frac{Q}{3} = \left( \frac{k_1 + k_2 + k_3}{3} \right) \delta_1 \quad (A2)$$

where

$P$  = average load per beam

$\delta_1$  = least deflection capacity of a group of three beams

$k_1$  = stiffness of a beam whose deflection capacity is  $\delta_1$

$k_2, k_3$  = stiffness of beams whose deflection capacities exceed  $\delta_1$

Equation (A2) shows how the desired output statistic  $P$  depends on input statistics of three beams chosen at random from a given input population.

Let

$$K = \frac{1}{3}(k_1 + k_2 + k_3) \quad (A3)$$

be the average stiffness of the beams in the structure, so that

$$P = K \delta_1 \quad (A4)$$

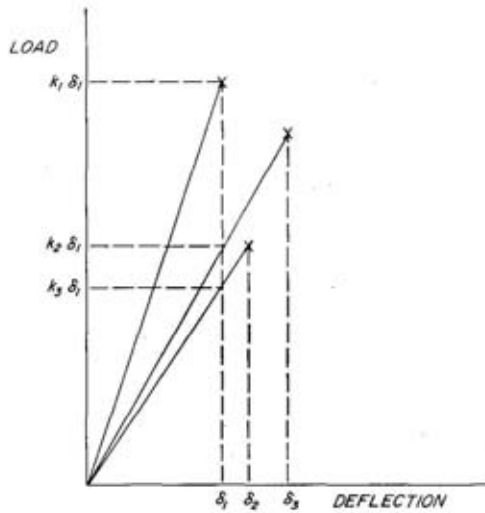


Figure A1.--Load deflection diagrams for three typical beams. Beam loads at first break of three-beam brittle-link structure are noted.

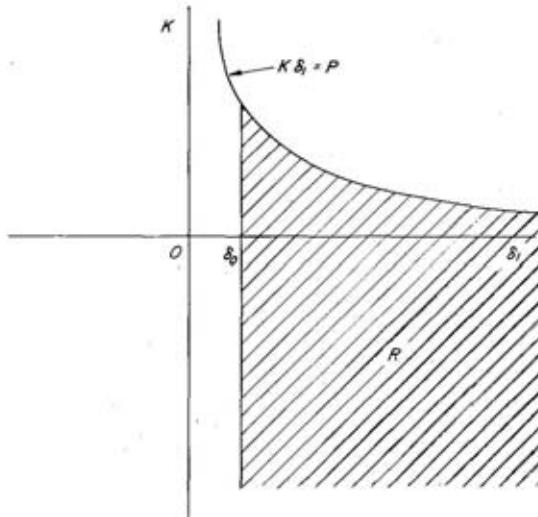


Figure A2.--Region R of equation (A9) illustrated. It is assumed here that  $\delta_1$  has a finite lower limit. Region R of equation (11) is similar, with  $\delta_1$  replaced by  $\delta$ .

Values of  $\underline{K}$  and  $\underline{\delta_1}$  are not known, but probabilistic statements about their values can be derived from the given bivariate distribution  $F_{in}(k, \delta)$ . Consider  $\underline{\delta_1}$  first. By definition,  $\underline{H(\delta)}$  is the probability of failure of a single beam at deflection  $\underline{\delta}$ .

Conversely,  $1 - H(\delta)$  is the probability of survival. The probability of joint survival of  $N$  beams is

$$1 - H_1(\delta_1) = [1 - H(\delta_1)]^N \quad (A5)$$

where  $H_1$  is the distribution of  $\delta_1$ . In other words,  $\delta_1$  is the first order statistic of a sample of size  $N$ , exactly as  $P$  was in the analysis of weakest-link structures in the body of the report. The PDF (probability density function) of  $\delta_1$  is

$$h_1(\delta_1) = N [1 - H(\delta_1)]^{N-1} h(\delta_1) \quad (A6)$$

Note how the terms in equation (A2) were defined. The stiffness values were made conditional to the value of  $\delta_1$ . This was done so that the probability of the joint occurrence of  $K$  and  $\delta_1$  could be written

$$P_r[K, \delta_1] = P_r[\delta_1] \cdot P_r[K | \delta_1] \quad (A7)$$

and the output CDF of  $P$  obtained from

$$\begin{aligned} G_{out}(P) &= P_r[K, \delta_1 \leq P] \\ &= \sum_R P_r[\delta_1] \cdot P_r[K | \delta_1] \end{aligned} \quad (A8)$$

where  $R$  is the set of all possible structures for which  $K, \delta_1 \leq P$ .

Let  $f(K; \delta_1)$  be the PDF of  $K$  given  $\delta_1$ . Then equation (A8) can be written

$$G_{out}(P) = \iint_R h_1(\delta_1) \cdot f(K; \delta_1) d\delta_1 dK \quad (A9)$$

where  $R$  is the region  $K, \delta_1 \leq P$ . See figure A2.

Consider the conditional PDF of  $K$  given  $\delta_1$ . For illustration, let  $N=3$ . The occurrence of a particular value of  $K$  is the joint occurrence of three independent events. Hence,

$$\begin{aligned} f(K; \delta_1) dK &\equiv P_r[K | \delta_1] \\ &= P_r[k_1 | \delta_1] \cdot P_r[k_2 | \delta_2 \geq \delta_1] \cdot P_r[k_3 | \delta_3 \geq \delta_1] \end{aligned} \quad (A10)$$

The probabilities on the right side of equation (A10) can be obtained from  $F_{in}$  using Bayes' theorem (9):

$$\begin{aligned}
 P_r[k_1 | \delta_1] &= \frac{P_r[k_1, \delta_1]}{\sum_{\text{all } k} P_r[k, \delta_1]} \\
 &= \frac{f_{in}(k_1, \delta_1) dk_1}{\int_{-\infty}^{\infty} f_{in}(k, \delta_1) dk} \\
 &\equiv p(k_1; \delta_1) dk_1
 \end{aligned} \tag{A11}$$

where  $p$  is so defined. This is the probability that a beam has stiffness  $k_1$ , given that its deflection capacity is  $\delta_1$ . Similarly,

$$\begin{aligned}
 P_r[k_2 | \delta_2 \geq \delta_1] &= \frac{\sum_{\delta \geq \delta_1} P_r[k_2, \delta]}{\sum_{\text{all } k} \sum_{\delta \geq \delta_1} P_r[k, \delta]} \\
 &= \frac{\int_{\delta_1}^{\infty} f_{in}(k_2, \delta) d\delta dk_2}{\int_{-\infty}^{\infty} \int_{\delta_1}^{\infty} f_{in}(k, \delta) d\delta dk} \\
 &\equiv q(k_2; \delta_1) dk_2
 \end{aligned} \tag{A12}$$

where  $q$  is so defined. This is the probability that a beam has stiffness  $k_2$ , given that its deflection capacity equals or exceeds  $\delta_1$ . Since beam 3 is characterized in the same way as beam 2,

$$P_r[k_3 | \delta_3 \geq \delta_1] = q(k_3; \delta_1) dk_3 \tag{A13}$$

Recalling equation (7), one sees that equations (A11) and (A12) permit  $p$  and  $q$  to be written in the form of equations (8), given in the body of the report.

Summing equation (A10), one obtains the CDF of K given  $\delta_1$  to be

$$F(K; \delta_1) = \sum_{\underline{S}} P_r[k_1 | \delta_1] \cdot P_r[k_2 | \delta_2 \geq \delta_1] \cdot P_r[k_3 | \delta_3 \geq \delta_1]$$

$$= \iiint_{\underline{S}} p(k_1; \delta_1) q(k_2; \delta_1) q(k_3; \delta_1) dk_1 dk_2 dk_3$$
(A14)

where S is the region  $\frac{1}{3}(k_1 + k_2 + k_3) \leq K$ . It can be shown that the right side of equation (A14) reduces to

$$F(K; \delta_1) = \int_{-\infty}^{3K} p * q * q(t; \delta_1) dt$$
(A15)

where the operation denoted by a star is the convolution as defined by equation (9). Generalizing to N beams and using the star exponent notation defined by equation (10), one obtains

$$F(K; \delta_1) = \int_{-\infty}^{NK} p * q^{*(N-1)}(t; \delta_1) dt$$
(A16)

Differentiation of equation (A16) produces the desired conditional PDF:

$$f(K; \delta_1) = N p * q^{*(N-1)}(NK; \delta_1)$$
(A17)

Finally, equations (A6) and (A17) maybe substituted into equation (A9) to produce

$$G_{out}^{(P)} = \iint_R N [1 - H(\delta_1)]^{N-1} h(\delta_1) N p * q^{*(N-1)}(NK; \delta_1) d\delta_1 dK$$
(A18)

The subscript on  $\delta_1$  may now be dropped. The derivation of equation (11) is then complete.

## **appendix B**

### Computer Simulation of Structural Tests

Consider a prototype structure shown in figure 1 in which the deck element has a finite nonzero stiffness. A five-beam structure was used in this computer simulation study. Figure B1 shows a free body diagram of the deck. On this figure, q is the distributed load in pounds per foot, a is the joist spacing, and R<sub>1</sub>

to  $R_5$  the forces exerted on the deck by the five support beams. Using linear elastic theory and equating the deck deflection to the joist deflection at each of the five joists, it can be shown that the five forces  $R_1$  to  $R_5$  satisfy the linear system shown in figure B2.

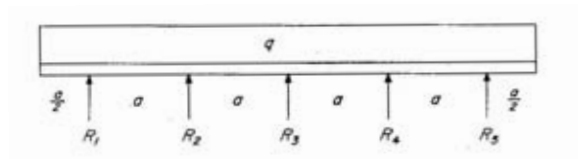


Figure B1.-Free body diagram of deck element.

$$\sum_j C_{ij} R_j = b_i q a, \quad i = 1, 5$$

$C_{11} = 480 + 3\rho_1$	$C_{31} = 48 + \rho_1$	$b_1 = 780$
$C_{12} = 216 - 4\rho_2$	$C_{32} = 8 - 2\rho_1$	$b_2 = 270$
$C_{13} = 64$	$C_{33} = \rho_3$	$b_3 = 58$
$C_{14} = 8$	$C_{34} = 0$	$b_4 = 5$
$C_{15} = \rho_5$	$C_{35} = 0$	$b_5 = 0$
$C_{21} = 192 + 2\rho_1$	$C_{4j} = 1, j = 1, 5$	
$C_{22} = 64 - 3\rho_2$	$C_{51} = 2$	
$C_{23} = 8$	$C_{52} = 1$	
$C_{24} = \rho_4$	$C_{53} = 0$	
$C_{25} = 0$	$C_{54} = -1$	
	$C_{55} = -2$	

Figure B2.--Linear system satisfied by the deck reactions.

In figure B2,

$$\rho_i = \frac{(EI)_{\text{deck}}}{(EI)_{\text{beam } i}} \cdot \frac{L^3}{a^3} \quad (B1)$$

Thus,

$$\rho_i = \frac{\text{Modal MOE}}{\text{MOE of beam } i} \cdot \rho \quad (\text{B2})$$

with  $\rho$  defined in the body of the report. Parameter  $\rho$  shall be used as a computer input variable specifying deck stiffness relative to the modal stiffness of the input population of beams.

The result of solving the linear system is of the form

$$R_i = r_i q a \quad (\text{B3})$$

where the  $r_i$  is the unit response so defined. As the load  $q$  is increased, the maximum stress  $\sigma_i$  in each beam increases in proportion to  $R_i$ . Call the proportionality constant  $\beta$ :

$$\sigma_i = R_i \beta \quad (\text{B4})$$

The criterion of failure is

$$\sigma_i \leq \text{MOR}_i, \quad i = 1, 5 \quad (\text{B5})$$

or

$$\beta r_i q a \leq \text{MOR}_i, \quad i = 1, 5 \quad (\text{B6})$$

and at first break

$$q_{\text{fail}} = \frac{1}{a\beta} \min_{i=1,5} \left( \frac{\text{MOR}}{r} \right)_i \quad (\text{B7})$$

The apparent MOR of the beams in the structure is, by definition,

$$\text{Apparent MOR} = \beta q_{\text{fail}} a \quad (\text{B8})$$

under the assumption that each beam carries an equal share of the load. Getting  $q_{\text{fail}}$  from equation (B7), equation (B8) becomes

$$\text{Apparent MOR} = \min_i \left( \frac{\text{MOR}}{r} \right)_i \quad (\text{B9})$$

Thus, the computer algorithm for getting the apparent MOR of a structure with five specified beams is:

1. Set up the linear system shown in figure B2 with  $q a = 1$ .

2. Solve it for the relative support reactions  $\underline{r}_1$ .
3. Divide MOR of each beam by corresponding  $\underline{r}$ .
4. Scan for the minimum value of MOR/ $\underline{r}$ .

In this manner, the destructive load test of a prototype structure was digitally simulated. The complete computer flow diagram is shown in the body of the report.

---

## **appendix c**

---

### Technique for Estimating Weibull Parameters

The Weibull distribution is of the form

$$G(x) = \begin{cases} 1 - e^{-\left(\frac{x-x_0}{\omega}\right)^m}, & x \geq x_0 \\ 0, & x \leq x_0 \end{cases} \quad (C1)$$

where  $x$  = a statistic such as strength or deflection capacity for which data are available

$x_0$  = lower limit of  $\underline{x}$

$\omega$  = a scaling parameter with the units of  $\underline{x}$

$m$  = a dimensionless shape parameter

The three parameters  $\underline{x}_0$ ,  $\omega$ , and  $\underline{m}$  are not uniquely associated with the gross shape of the distribution, that is, slight perturbations in the extremes of the distribution which leave the gross shape essentially the same can only be produced by large changes in the three parameters. Putting it another way, a change in one of the parameters can be compensated by suitable readjustment of the other two in such a way that the gross shape of the distribution remains unchanged except in the extremes. For this reason, maximum likelihood estimates of the parameters are not very meaningful; they are too dependent upon extreme values in the data. Omission of a few low data points can yield entirely different maximum likelihood estimates of the three parameters which nevertheless produce a distribution with the same overall shape.

The only way to escape this inherent redundancy of the parameters is to have either (a) sufficient data to establish the high and low tails with confidence, or (b) an independent estimate of one of the parameters by a criterion other than

goodness of fit. A method is presented here for obtaining  $\underline{m}$  and  $\underline{\omega}$  from goodness of fit once  $\underline{x}_0$  has been specified. If there are sufficient data to choose  $\underline{x}_0$  by goodness of fit also, the method can be iterated with  $\underline{x}_0$  adjusted by trial. However,  $\underline{x}_0$  will usually need to be chosen on the basis of other considerations. Its interpretation as a lower limit may be a guide.

Let the data in a sample of size  $\underline{N}$  be ordered according to  $x$ . That is,

$$\underline{x}_1 < \underline{x}_2 < \underline{x}_3 < \dots < \underline{x}_N \quad (C2)$$

Associate with each  $\underline{x}_i$  a corresponding cumulative frequency  $\underline{G}_i$

$$\underline{G}_i = \frac{i}{N}, \quad i = 1, N \quad (C3)$$

For good fit,  $\underline{G}(\underline{x}_i)$  and  $\underline{G}_i$  should be made as much alike as possible, in some sense. Rather than minimize the difference directly, it is more convenient to first employ a transformation which linearizes equation (C1) and then fit a straight line by least squares.

Solving equation (C1) for  $x - x_0$  yields

$$x - x_0 = \omega \left[ \log \frac{1}{1 - G} \right]^{1/m} \quad (C4)$$

Taking logarithms of both sides of this equation yields

$$\log(x - x_0) = \log \omega + \frac{1}{m} \log \log \frac{1}{1 - G} \quad (C5)$$

which is of the form

$$Y(X) = A + BX \quad (C6)$$

where  $X = \log \log \frac{1}{1 - G}$

$A = \log \omega = \text{intercept}$

$B = \frac{1}{m} = \text{slope}$

Thus, the pairs  $(\underline{x}_i, \underline{G}_i)$  are transformed to the pairs  $(Y_i, X_i)$  where

$$\begin{aligned} Y_i &= \log(x_i - x_0), \quad i = 1, N \\ X_i &= \log \log \frac{1}{1 - G_i} \\ &= \log \log \frac{N}{N - i}, \quad i = 1, N \end{aligned} \quad (C7)$$

The straight line given by equation (C6) can now be fitted to the data given by transformation (C7). After  $\underline{A}$  and  $\underline{B}$  have been found by least squares,  $\underline{m}$  and  $\underline{\omega}$  are obtained from

$$m = \frac{1}{B}$$

$$\omega = e^A$$
(C8)

When  $\underline{x}_0$  is also to be determined by goodness of fit, one may plot the transformed data  $(Y_i, X_i)$  in the X-Y plane and adjust  $\underline{x}_0$  for the straightest possible line. In doing so, low extreme data should be censored since the logarithmic transformation exaggerates the low range. It is always necessary to censor the largest value, since  $\underline{X}_N$  is infinite. One could avoid this awkward situation by modifying the definition of  $\underline{G}_1$  if desired. Since the judicious censorship of low-extreme data is vital to the success of this technique, it is advisable to employ a computer, a plotter, and a human in a closed feedback loop when using the method. In fact, it seems inadvisable ever to estimate Weibull parameters entirely automatically, by any method, in view of the inherent redundancy of parameters discussed above.

### Example

Consider the 80 pieces of Construction Grade Douglas-fir known as case 3 in the body of this report. Here the deflection capacity  $\underline{\delta}$  will play the role of  $\underline{x}$ . Figure C1 shows the transformed data plotted twice, once with  $\underline{\delta}_0$  equal to

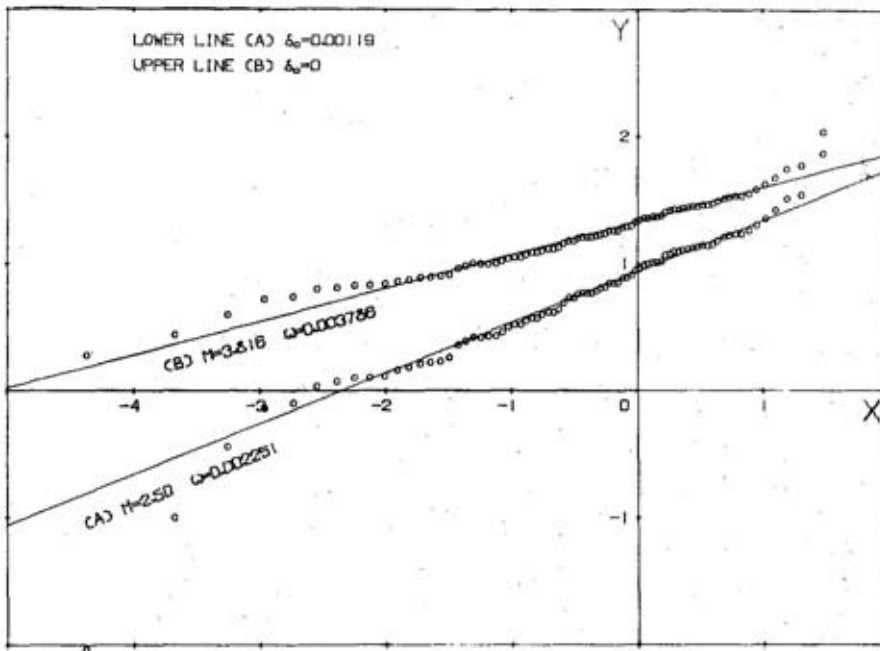


Figure C1.--Transformed data for deflection capacity, case 3. Two choices for  $\underline{\delta}_0$  are compared, and each transformed set is fitted with a straight line by least squares. Parameters obtained from the fit are shown with the line.

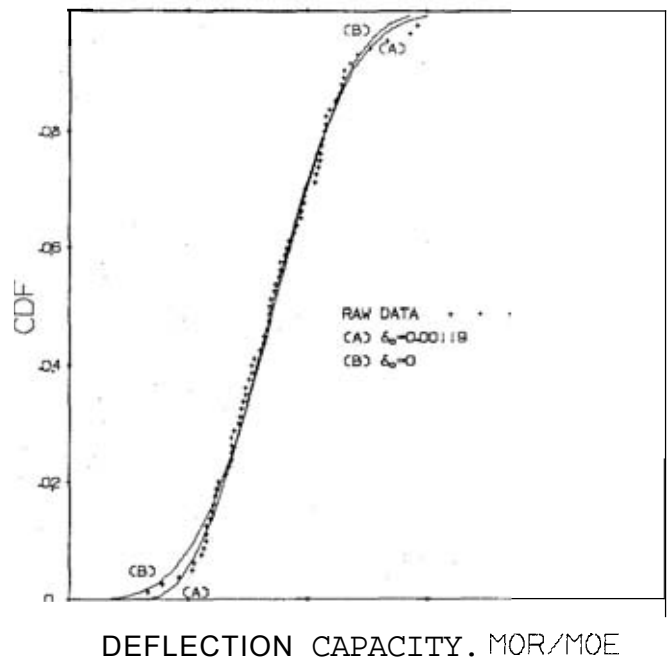


Figure C2.--Comparison of two Weibull distributions fitted to raw data for deflection capacity, case 3. Each fit corresponds to a particular choice for  $\delta_0$ .

0.00119 (case 3a) and once with  $\delta_0$  equal to zero (case 3b). In each case the first three points were censored before fitting the least squares line shown. Resulting values of  $\underline{m}$  and  $\underline{\omega}$  are given on the figure. Figure C2 shows the same data in the original plane with both fitted distributions drawn for comparison. As may be seen, there is not much reason to prefer one fit to the other. In the midrange where data are most plentiful, the two fits agree. In the body of the report, reasons are adduced for preferring case 3a to case 3b, because it seems to perform better in the brittlest-link algorithm, equation (20). This was revealed by the "N=1 test" of the algorithm in which the number of beams was set equal to one and the result compared with the raw-strength data of individual beams. See figures 13 and 14.

---

## appendix D

---

### Notation

a	Deck span, <b>i.e.</b> , distance between adjacent beams
CDF	Abbreviation for Cumulative Distribution Function
EI	Flexural rigidity, pound-inch <sup>2</sup>
$f(\underline{K}; \underline{\delta}_1)$	PDF of $\underline{K}$ given $\underline{\delta}_1$

$F(K; \delta_1)$	CDF of $\underline{K}$ given $\delta_1$
$f_1(\delta), f_2(k)$	Marginal PDF's of $f_{in}(k, \delta)$ . See equation (12).
$f_{in}(k, \delta)$	Bivariate PDF of input population of beams
$F_{in}(k, \delta)$	Bivariate CDF of input population of beams
$G_{in}$	Strength CDF of input population of beams
$G_{out}$	Strength CDF of output population of structures
$h(\delta)$	Marginal PDF of $f_{in}(k, \delta)$ . See equation (7).
$H(\delta)$	Marginal CDF of $F_{in}(k, \delta)$
$h_1(\delta_1)$	PDF of first order statistic $\underline{\delta}_1$
$H_1(\delta_1)$	CDF of first order statistic $\underline{\delta}_1$
$k$	Beam stiffness, pounds per inch. Proportional to MOE.
$K$	Average stiffness of $\underline{N}$ beams
$L$	Beam span length
LSI	Abbreviation for Load Sharing Increase, defined by equation (22).
$m$	Weibull parameter. See equations (3) and (18).
MOE	Abbreviation for Modulus of Elasticity
MOR	Abbreviation for Modulus of Rupture
$N$	Number of beams in structure
$\left. \begin{matrix} p(k; \delta) \\ q(k; \delta) \end{matrix} \right\}$	Defined by equations (8)
$P$	Beam strength, pounds. Proportional to MOR
$P_q$	Lower limit of $\underline{P}$ for a population
PDF	Abbreviation for Probability Density Function
$\Pr [A B]$	Notation for "probability of $\underline{A}$ given $\underline{B}$ "
$Q$	Total load on structure, pounds
$Q(t)$	Standard normal CDF; error function

$\delta$	Deflection capacity of a beam, inches
$\delta_0$	Lower limit of $\underline{\delta}$ for a population
$\delta_1$	Least $\underline{\delta}$ in a sample of size $N$
$\mu$	Mean value of stiffness $\underline{k}$
$\rho$	Relative deck stiffness. See equation (21).
$\sigma$	Standard deviation of stiffness $\underline{k}$
$\omega$	Weibull parameter. See equations (3) and (18)